# Hedgehog-GLI Signaling Inhibition

# Suppresses Tumor Growth in Squamous Lung Cancer

by

Lingling Huang

Department of Pharmacology and Cancer Biology
Duke University

Date:_____

Approved:

_____
Mark Onaitis, Co-supervisor

_____
David Kirsch, Co-supervisor

_____
Xiao-Fan Wang

_____
Daniel Wechsler

Dissertation submitted in partial fulfillment of
the requirements for the degree of Doctor
of Philosophy in the Department of
Pharmacology and Cancer Biology in the Graduate School
of Duke University

2014

ABSTRACT

Hedgehog-GLI Signaling Inhibition

Suppresses Tumor Growth in Squamous Lung Cancer

by

Lingling Huang

Department of Pharmacology and Cancer Biology
Duke University

Date:_____

Approved:

_____
Mark Onaitis, Co-supervisor

_____
David Kirsch, Co-supervisor

_____
Xiao-Fan Wang

_____
Daniel Wechsler

An abstract of a dissertation submitted in partial
fulfillment of the requirements for the degree
of Doctor of Philosophy in the Department of
Pharmacology and Cancer Biology in the Graduate School of
Duke University

2014

# Abstract

Lung squamous cell carcinoma (LSCC) comprises ~30% of non-small cell lung cancers, and currently lacks effective targeted therapies. Previous immunohistochemical and microarray studies reported overexpression of Hedgehog (HH)-GLI signaling components in LSCC. However, they addressed neither the tumor heterogeneity nor the requirement for HH-GLI signaling. Here, we investigated the role of HH-GLI signaling in LSCC, and studied the therapeutic potential of HH-GLI pathway suppression.

Gene expression datasets of two independent LSCC patient cohorts were analyzed to study the activation of HH-GLI signaling. Four human LSCC cell lines were examined for HH-GLI signaling components. Cell proliferation and apoptosis were assayed in these cells after blocking the HH-GLI pathway by lentiviral-shRNA knockdown or small molecule inhibitors. Xenografts in immunodeficient mice were used to determine the *in vivo* efficacy of GLI inhibitor GANT61.

In both patient cohorts, we found that activation of HH-GLI signaling was significantly associated with the classical subtype of LSCC. *GLI2* expression level was significantly higher than *GLI1*, and displayed strong positive correlations with the prominent markers for the classical subtype (*SOX2*, *TP63* and *PIK3CA*) on chromosome 3q. In cell lines, genetic knockdown of SMO produced minor effects on cell survival, while GLI2 knockdown significantly reduced proliferation and induced extensive

apoptosis. Consistently, the SMO inhibitor GDC-0449 resulted in limited cytotoxicity in LSCC cells, whereas the GLI inhibitor GANT61 was very effective. Importantly, GANT61 demonstrated specific *in vivo* anti-tumor activity in xenograft models of GLI-positive cell lines.

Taken together, we report SMO-independent regulation of GLI in LSCC, and demonstrate an important role for GLI2 in LSCC. Different from standard-of-care chemotherapy or small molecule inhibition of kinase signaling cascades, we present a novel and potent strategy to treat a subset of LSCC patients by targeting the GLI transcriptional network.

# Dedication

I dedicate my dissertation to my parents, Chaohai Huang and Xi'e Mo, for their endless love and unconditional support in my pursuit of academic excellence.

I also dedicate my work to Mark Onaitis and Christian Parobek, who have provided my unlimited support as mentors and walked me through the entire doctorate program towards a new career.

# Contents

# List of Tables

# List of Figures

# List of Abbreviations

| | |
|---|---|
| ATO | Arsenic Trioxide |
| BSA | Bovine serum albumin |
| CCLE | Cancer Cell Line Encyclopedia |
| CCND1 | Cyclin D1 |
| cDNA | complementary DNA |
| DDR2 | Discoidin Domain Receptor Tyrosine Kinase 2 |
| DHH | Desert Hedgehog |
| DNA | Deoxyribonucleic Acid |
| FBS | Fetal Bovine Serum |
| FGF | Fibroblast Growth Factor |
| FGFR1 | Fibroblast Growth Factor Receptor 1 |
| GAPDH | Glyceraldehyde-3-phosphate Dehydrogenase |
| GLI | GLI family zinc finger |
| GPCR | G-protein coupled receptor |
| HH | Hedgehog |
| HHIP | Hedgehog interacting protein |
| HMG | High Mobility Group |
| IHC | Immunohistochemistry |

| | |
|---|---|
| KEAP1 | Kelch-like ECH-associated protein 1 |
| IHH | Indian Hedgehog |
| LSCC | Lung squamous cell carcinoma |
| mRNA | messenger RNA |
| mTOR | mechanistic target of rapamycin |
| NFE2L2 | Nuclear Factor, Erythroid 2-like 2 |
| NSCLC | Non-small cell lung cancer |
| MEK | Mitogen-Activated Protein Kinase Kinase |
| PARP | Poly (ADP-ribose) polymerase 1 |
| PCR | Polymerase Chain Reaction |
| PI3K | Phosphatidylinositol 3-kinase |
| PIK3CA | Phosphatidylinositol-4,5-bisphosphate 3-kinase, catalytic subunit alpha |
| PKA | Protein Kinase A |
| PTCH | Patched |
| PTEN | Phosphatase and tensin homolog |
| RAS | RAS protein family of small GTPase |
| RNA | Ribonucleic Acid |
| SCLC | Small cell lung cancer |
| SD | Standard Deviation |

| | |
|---|---|
| SHH | Sonic Hedgehog |
| SMO | Smoothened |
| SOX2 | Sex determining region Y-box2 |
| SUFU | Suppressor of fused homolog (Drosophila) |
| TBST | Tris-Buffered Saline and Tween 20 |
| TCGA | The Cancer Genome Atlas |
| TP63 | Tumor Protein p63 |
| TTF-1/ NKX2-1 | Thyroid Transcription Factor 1 |
| UNC | University of North Carolina |
| VEGF | Vascular Endothelial Growth Factor |

# Acknowledgements

Graduate school experience in a foreign country has been difficult yet memorable. Although there were thousands of times that I questioned myself whether pursing a PhD in science was a correct decision, I have been enjoying a truly wonderful journey in the past five years. It is obviously not possible without the heartfelt understanding and persistent support from numerous people.

First of all, my deepest gratitude goes to my thesis advisor Dr. Mark Onaitis, who plays a dual role as a mentor and a parent, for his tremendous mentorship, support, and trust throughout each footstep of my professional and personal development. His enthusiasm for both basic and clinical research, open mind about new ideas and willingness of teaching have made him the perfect person to learn from and work with. Frustration and disappointment are inevitable in studying biosciences, and I sincerely appreciate his understanding and encouragement when I encounter difficulties. Although he is extremely busy as a thoracic surgeon, he has always been willing to listen to me, and encourage me to pursue the projects that I am truly interested in. He fully demonstrates his trust on me by offering me freedom and independence, so that I have been able to hone my problem-solving skills. He also provides generous support for my conference travels, through which I was able to see a bigger world of science and set up a higher standard for myself. He has also been important as a parent when I live

thousands of miles away from my family. I truly appreciate his understanding and tolerance of my occasional childish emotions, as well as his wisdom in guiding me to make life-changing decisions. I would have never accomplished this dissertation without his optimism, patience and support. I hope that I will become such an excellent physician-scientist as he is in the future.

Different from most of the graduate students, I have a more complicated experience since I have been working very closely to multiple laboratories inside and outside Duke University. I would like to express my thanks to these labs that have created such an efficient, inspiring, and supportive atmosphere for me to work in: Onaitis lab, Stripp lab, Kirsch lab, Hayes lab, Kornbluth lab, Wang lab, and Yang lab. Particularly, I want to thank Vonn Walter in Hayes lab, who has collaborated with us and helped us with genomic analysis. My deeply appreciation also goes to Zhizhong Li, Wanli Tang, Hui Wang, Bofu Huang, Chen Chen, Liguo Zhang, Meng He, Nai-jia Huang and Jordan Blum. They generously share their valuable experience and reagents, patiently teach me to conduct new experiments and help me solve many technical problems. Connections with these talented young scientists have become an unforgettable and integral part of my graduate school experience at Duke. I also would like to thank Liaxia Luo, Jing Zhang and Xia Xu for animal study, as well as Nicholas Manzo and Brian Brockway who have been kindly sharing their expertise in cell

culturing, microscope and immunostaining, and have provided insightful discussion for my projects.

I also want to give sincere gratitude to my committee members, David Kirsch, Xiao-Fan Wang, and Daniel Wechsler for their valuable advice and suggestions. As my co-advisor, Dr. David Kirsch has offered me tremendous mentorship, guidance and help with his broad knowledge and willingness to train young scientists. My rotation in Kirsch lab is a valuable experience that provided me with sufficient scientific trainings, and many aspiring young researchers as friends. In addition, I also want to thank Dr. Dong Liu, who was my research advisor at Tsinghua University. The two-year research training in Liu lab has opened the door of biological science to me, and Dr. Liu has been a great example of scientists full of curiosity for research and life.

My parents, Chaohai Huang and Xi'e Mo, have always been my bedrock with their unconditional love and persistent support, no matter how far I go and how much I achieve. Their understanding, trust, and pride in me have been my ultimate impetus to pursue my dreams and life goals. My dear friends all over the world, Wanli Tang, Xixi Chen, Guo Li, Zhao Chen, Xiaolei Li, Danqing Zhou, Hua Wei, Xue Bai, Zheng Zeng, also weave a continuous friendship for me, protecting me from loneliness.

Finally, I want to express my deeply appreciation to Christian Parobek, who is the most important American friend to me. Although younger than me, he has actually been my mentor in career development and a big brother in my life with his beautiful

heart, valuable friendship, kindhearted patience and endless positive energy. He is the one who is willing to listen to me, who understands my happiness, frustration and fear, who I can always trust and rely on, who guides me to discover my potential, encourages me to pursue a seemingly impossible career goal and walks alongside of me step by step towards a completely new era of professional development. He may not fully realize how much he has changed my life, just as he may not know how wonderful he is. I truly believe that he will definitely become an excellent physician (and a great scientist if he also wants to), and I wish one day I can become such a good person and good doctor like him.

I cannot imagine my life without these important people, who make me feel that I am loved, trusted and supported.

# 1. Background and Overview[1]

## *1.1 Lung squamous cell carcinoma*

### 1.1.1 General

Lung cancer is the leading cause of cancer-related death worldwide. Non-small cell lung cancer (NSCLC) comprises ~80% of all lung cancer cases, which includes three major histological types: squamous cell carcinoma (20~30%), adenocarcinoma (~40%) and large cell carcinoma (~10%). Squamous cell carcinoma (SCC) is associated most strongly with cigarette smoking. Archetypically, SCC commonly occurs in the main stem, lobar, and segmental bronchi as central airway tumors, while the frequency of peripheral SCC is greatly increasing recently. Clinically, patients with central SCC tumors can present with cough shortness of breath, and fever secondary to atelectasis and postobstructive pneumonia. Hemoptysis is an important feature that can be related to both location and an increased proclivity towards cavitation. Compared with lung adenocarcinoma, SCC tends to be locally aggressive with less frequent metastasis to distant organs (1).

[1] The main part of this dissertation has been published in the journal *Clinical Cancer Research* (Huang et al., 2014). To reproduce the contents, including the figures, from the published article in this dissertation is retained as the author's non-exclusive right and permitted by the American Association for Cancer Research (AACR) Publications policy.

### 1.1.2 Pathologic Features

Histologically, well differentiated LSCCs are characterized by keratinization, intercellular bridges and pearl formation (Figure 1). Tumor cells are usually large with abundant dense cytoplasm, irregular hyperchromatic nuclei and small nucleoli. These features can be present only focally in poorly differentiated LSCCs (1). Immunohistochemical (IHC) staining for Tumor Protein p63 (TP63) and Thyroid Transcription Factor 1 (NKX2-1/ TTF-1) has been used to determined histology in challenging specimens in order to guide further molecular tests. TP63 is a transcription factor essential for stratified squamous epithelium development. TTF-1 is a protein that regulates transcription of genes specific for the thyroid, lung and diencephalon. LSCC commonly expresses TP63, and is negative for TTF-1.

### 1.1.3 Clinical treatments

Management of NSCLCs has changed dramatically during the past decade due to the discovery of molecular oncogenic mechanisms. Although targeted therapies resulted from these discoveries continue to improve clinical care, the benefit to patients has largely favored those with lung adenocarcinoma. In contrast, progress in LSCC treatment has been modest, and targeted therapeutics are still lacking. Chemotherapy remains the first-line treatment for most patients with stage IV NSCLC, and optimal regimens are now guided by histology. Platinum-based regimens with pemetrexed, bevacizumab (a monoclonal antibody against VEGF), or both are reasonable first-line

options for patients with non-squamous NSCLC. No agents are currently approved specifically for the treatment of LSCC. In a preplanned subgroup analysis based on histology, the combination of cisplatin and gemcitabine was associated with a 1.4-month survival advantage compared with the combination of cisplatin and pemetrexed (10.8 months with gemcitabine versus 9.4 months with pemetrexed). Therefore, the standard treatment remains a platinum doublet with a drug other than pemetrexed (2).

## *1.2 Molecular carcinogenesis of LSCC*

### 1.2.1 Oncogenic gene alterations

In contrast to adenocarcinoma, druggable molecular drivers have not been identified in LSCC, and the current targeted agents for lung adenocarcinoma are largely ineffective for treating LSCC patients. Gradually, oncogenic alterations have been described in LSCC, including *SOX2* amplification, dysregulation of the KEAP-NFE2L2 pathway, aberrant PI3K pathway activity, *FGFR1* amplification, and *DDR2* mutation (1).

SOX2, short for sex determining region Y-box2, is a High Mobility Group (HMG) transcription factor, essential for stem cell pluripotency. Sox2 is required for precise branching morphogenesis and epithelial cell differentiation during lung development (3, 4), as well as the self-renewal ability of basal cells after injury (5). Recently, *SOX2* is reported to be an amplified lineage-survival oncogene in human LSCC (6, 7). Sox2 is also upregulated in squamous cell carcinomas of different organ sites (6, 8). *SOX2* knockdown reduces cell proliferation of *SOX2*-overexpressing LSCC cell lines *in vitro*

(6). Lung–specific *Sox2* overexpression in mouse models is tumorigenic (9). These studies collectively demonstrate a critical role of SOX2 in LSCC.

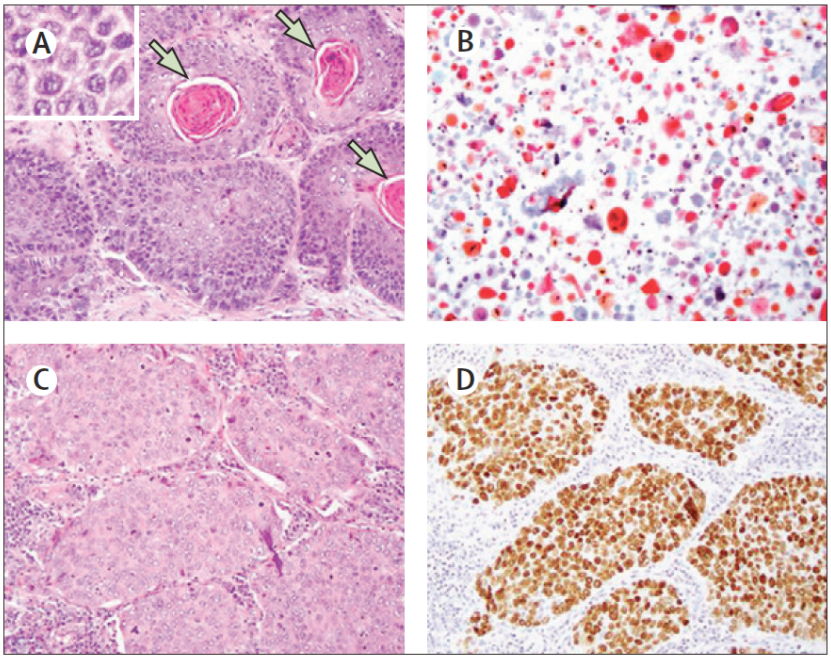


**Figure 1: Pathological features of LSCC**

A. Classic morphological features of LSCC: keratinized cells forming cellular pearls (arrows) and intercellular bridges (inset). B. Cytoplasmic keratinization in well differentiated LSCC (bright red, orange and blue). C. Examples of a poorly differentiated area of LSCC, where classic morphological differentiation is lacking. D. TP63 staining in poorly differentiated LSCC. (Adapted from Drilon et al. (1))

The KEAP-NFE2L2 pathway is important in regulating cellular responses to oxidative and xenobiotic stress. Under stressful condition, modified KEAP1 decreases the degradation of NFE2L2, which is the transcriptional activator for cytoprotective genes in elimination of reactive oxygen species, xenobiotic metabolism, and drug transport. Mutations in the coding region of *NFE2L2* occur predominantly in LSCC patients and are associated with a history of smoking (10, 11). Cells with *NFE2L2* mutations display constitutive induction of drug efflux pumps and cytoprotective enzymes, and NFE2L2 knockdown abrogates these effects (10).

The phosphatidylinositol 3-kinase (PI3K) pathway plays a central role in cell survival, metabolism, motility and angiogenesis. Several studies show that abnormal PI3K signaling is more common in LSCC than in lung adenocarcinoma. Amplification of *PIK3CA*, the gene encoding the catalytic subunit of PI3K, is prevalent in LSCC (12-14). *PTEN* is a tumor suppressor gene that negatively regulates the PI3K-AKT-mTOR axis, and loss of PTEN function that results in increased pathway activity has been reported in LSCC (15).

The Fibroblast Growth Factor Receptor (FGFR) is a transmembrane receptor tyrosine kinase that participates in the regulation of embryonic development, cell proliferation, differentiation and angiogenesis. The FGFR family has four members and binds up to 22 FGF ligands. Frequent and focal *FGFR1* amplifications are reported in LSCC specimen (16, 17). Cell lines endogenously harboring *FGFR1* amplification show

growth dependency on this amplification, suggesting *FGFR1* as a potential therapeutic target in LSCC.

The Discoidin Domain Receptor (DDR) is a receptor tyrosine kinase that regulates cell adhesion, proliferation, and extracellular remodeling upon binding to its endogenous ligand, collagen. *DDR2* mutation presents in 4% of LSCC. Gain-of-function mutation of *DDR2* can be inhibited by dasatinib, a multi-kinase inhibitors against both DDR1 and DDR2 (18), raising the treatment possibility for molecularly selected patients with LSCC.

### 1.2.2 mRNA expression subtypes

LSCC has broad morphologic, genetic and clinical heterogeneity. Currently, no subclassification adequately addresses this variability and LSCCs are treated as a single disease. Recent analysis of gene expression of resected tumors has classified LSCC into four mRNA expression subtypes, defined as classical (36%), primitive (15%), secretory (24%) and basal (25%) (19, 20). The four subtypes have significantly different survival outcomes, patient populations, and biological characteristics. The primitive subtype has the worst overall survival and relapse-free survival in all stages of LSCC, whereas the other three subtypes have similar outcomes. Genes associated with cellular proliferation, as well as DNA repair and RNA processing, are overexpressed in the primitive subtype (19). The classical subtype, which has the greatest concentration of smokers and heaviest smokers, exhibits overexpression of genes related to xenobiotic metabolism, which

detoxifies foreign chemicals. The classical subtype is also characterized by alterations in *KEAP1*, *NFE2L2* and *PTEN*, as well as the greatest overexpression of the three known oncogenes on chromosome 3q: *SOX2*, *TP63* and *PIK3CA* (20). Immune response related genes and lung secretory cell markers are overexpressed in the secretory subtype. The basal subtype shows an enrichment of genes related to cell adhesion and epidermal development (19). The oncogenic drivers and potential cells of origin of tumors within these subtypes are likely different. Although the subtypes may help to stratify patients for more precise prognosis and targeted therapies, the practical application of these expression subtypes in clinical care has not been determined.

## *1.3 Hedgehog-GLI signaling*

### 1.3.1 Canonical Hedgehog-GLI signaling

As illustrated in Figure 2, canonical Hedgehog (HH)-GLI signaling is initiated by the binding of HH ligands (Sonic, Indian and Desert Hedgehog) to a 12-transmembrane receptor Patched (PTCH). The binding of HH to PTCH relieves the catalytic inhibition of Smoothened (SMO), a 7-transmembrane G-protein coupled receptor (GPCR)-like signal transducer. SMO de-repression triggers a series of intracellular events, resulting in the activation of downstream target genes through the transcriptional effectors GLI1, GLI2 and GLI3 (21). The GLI effectors are regulated by complex mechanisms at both the transcriptional and post-translational levels. They have activator and repressor functions that are defined only partially and can respond to combinatorial and cooperative GLI

activity (22). GLI2 appears to be the primary activator of HH signaling in cancer, with GLI1 as a transcriptional target of GLI2 (23-25). GLI2 and GLI1 also induce transcription of overlapping and distinct sets of downstream target genes (26). Several components of the HH pathway (PTCH, GLI1, GLI2, HHIP) are GLI transcriptional targets that induce positive or negative feedbacks. GLI targets mediate various cellular responses, notably enhanced cell proliferation and survival by upregulating D-type cyclins and anti-apoptotic proteins (27-29).

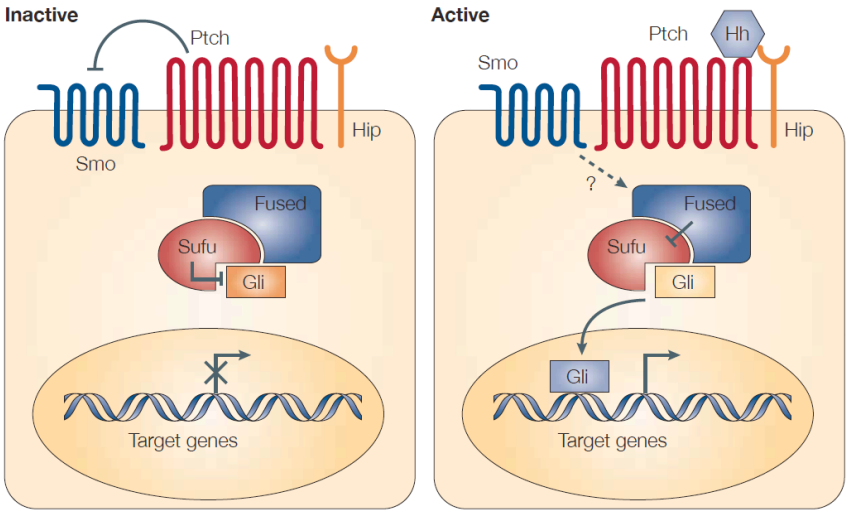


**Figure 2: Ligand-dependent activation of canonical HH-GLI signaling**

(Adapted from di Magliano et al. (21))

### 1.3.2 Non-canonical Hedgehog-GLI signaling

Constitutive activation of HH-GLI signaling, which may be caused by ectopic expression of SHH ligand, loss-of-function mutations of PTCH or SUFU, constitutively active SMO, and overexpression of GLI, has been reported to be tumorigenic. In addition, PI3K/AKT and RAS-MEK signals have been described as non-canonical HH-GLI activators in a context-dependent manner. Studies show that PI3K-depedent Akt positively regulates Shh-Gli signaling by controlling Protein Kinase A (PKA)-mediated Gli2 inactivation (30). While active SHH-GLI signaling in the matrix of human hair follicles is required for proliferation of melanocytes, oncogenic Ras-induced melanomas in transgenic mice express Gli1 and require Gli signaling both *in vitro* and *in vivo* for growth and metastasis. Endogenous Ras-Mek and Akt signaling also regulate the nuclear localization and transcriptional activity of GLI1 in melanoma (31). In transgenic mouse model of pancreatic ductal adenocarcinoma, Gli transcription is decoupled from Shh-Ptch-Smo axis and is regulated by TGF-β and Kras. Gli activity is required both for survival and the Kras-mediated transformed phenotypes of cultured pancreatic cancer cells (32). HH-GLI signaling also cross-talks with other oncogenic pathways, forming a complex cellular network.

### 1.3.3 Hedgehog-GLI signaling in lung development

HH-GLI signaling plays a critical role in lung morphogenesis. *Shh* ligand is specifically expressed in the budding airway epithelium during lung embryogenesis,

which is required for branching morphogenesis and epithelial-mesenchymal interaction (33). Shh-deficient mice exhibit hypoplastic lungs and severe branching defects, whereas overexpression of Shh results in increased cell proliferation to a lung containing abundant mesenchyme and not functional alveoli (34, 35). Mutations in the *Gli* genes give rise to various lung and foregut defects. While *Gli1* is dispensable for lung development in the presence of other *Gli* genes (36), *Gli2*$^{-/-}$ mutant lung exhibits lobe hypoplasia, narrowing of the trachea and esophagus (37). Compound mutants lacking both *Gli2* and *Gli3* are severely defective in upper foregut structures lacking lung, trachea, and esophagus (37). While these findings point to the importance of HH-GLI signaling in lung development, the functional involvement of this pathway in adult lung and lung cancer is less understood.

### 1.3.4 Hedgehog-GLI signaling in airway repair and small cell lung cancer

Dysregulation of the HH-GLI pathway has been implicated in carcinogenesis, maintenance of tumor progenitor cells and tumor-stromal interaction in a variety of cancers (38). Despite its importance during lung morphogenesis, HH-GLI signaling remains largely quiescent in adult lung homeostasis. Adult lung airway epithelium rarely proliferates unless injured. In a mouse model of acute airway repair, when Clara cells in the distal conducting airways are depleted by systemic naphthalene administration, widespread activation of the Shh-Gli pathway is observed in the increased neuroendocrine cells in the regenerating airway epithelium (39). Small cell

lung cancer is (SCLC) an aggressive, highly lethal malignance with primitive neuroendocrine features. Analysis of SCLC tissues reveals expression of SHH and GLI1. SCLC xenografts in nude mice demonstrate SHH-expressing cells adjacent to GLI1-expressing cells, and suppression of SHH-GLI signaling by SMO antagonist, cyclopamine, inhibits growth of SCLC xenografts in nude mice (39). In a transgenic mouse model in which deletion of Rb1 and p53 in adult lung epithelium induces SCLC, Hh-Gli signaling is found to be activated in SCLC cells independent of lung microenvironment. Constitutively active SMO enhances the survival and clonogenicity of human SCLC *in vitro*. While constitutive activation of SMO promotes the initiation and progression of mouse SCLC *in vivo*, genetic deletion of SMO from *Rb1* and *p53* dual mutant lung epithelial cells strongly suppresses SCLC initiation and progression (40). Moreover, pharmacological blockage of HH-GLI signaling with SMO inhibitor suppresses both mouse and human SCLC growth, most notably following chemotherapy (40). Taken together, these studies demonstrate a crucial role of HH-GLI signaling in the development and maintenance of SCLC, and suggest HH-GLI inhibition as a therapeutic strategy to treat patients with SCLC.

### 1.3.5 Hedgehog-GLI signaling in LSCC

Although the involvement of HH-GLI signaling in small-cell lung cancer is well established, the role of this pathway in non-small cell lung cancer remains poorly understood. However, multiple lines of evidence point to the potential importance of

HH-GLI signaling in LSCC. As shown in Figure 3, immunohistochemical (IHC) studies in patient specimens report the overexpression of HH signaling components (SHH, PTCH, SMO, GLI1 and GLI2) in LSCC, but absent from the adjacent non-neoplastic lung parenchyma (41, 42). High activation of the HH-GLI pathway defined by the intensity of IHC staining is observed in approximately 27% of LSCC. Analysis of three published microarray datasets identifies hyperactive HH signaling in LSCC in comparison to normal lung tissues (43). GLI-mediated HH signaling has been implicated in squamous cancer of other organs, including cancer of the oral mucosa and esophagus (44-46). Despite these studies, very little is known regarding the specific role of HH signaling in regulation of cellular survival and proliferation in LSCC.

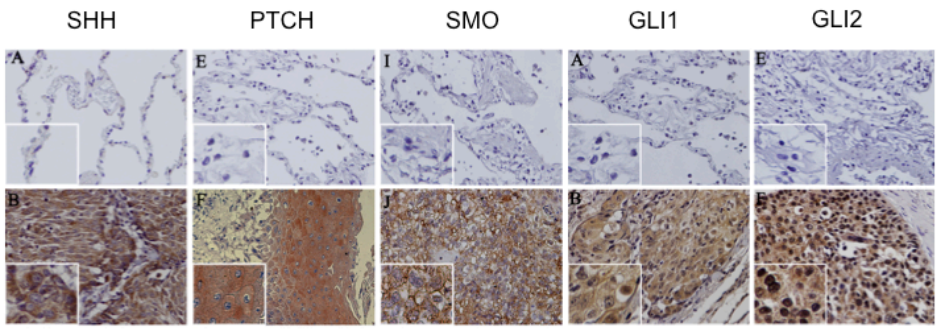


**Figure 3: IHC staining of HH signaling components in LSCC**

Upper panel: negative staining of HH components in alveolar epithelium and interstitium of adjacent non-neoplastic lung parenchyma. Bottom panel: Increased staining of indicated HH components in LSCC. (Adapted from Gialmanidis et al. (41))

### 1.3.6 Inhibitors of Hedgehog-GLI signaling

Targeted inhibitors of the HH pathway have become available recently. Because of its accessibility on the membrane and its importance in regulation of the pathway, SMO has been the primary focus in the development of small molecule inhibitors of the HH pathway. Cyclopamine, a natural alkaloid derivative, represents the first member of small chemical compounds that specifically inhibits SMO by binding to its heptahelical bundle. However, the difficulty to synthesize cyclopamine in large quantities makes it not applicable as a therapeutic agent. GDC-0449 (vismodegib; Genentech) is an orally administered agent that selectively suppresses SMO activity and subsequent downstream signaling. It is the first SMO inhibitor to progress to clinical trials and has recently been approved for use as a first-line treatment in advanced unresectable basal cell carcinoma. Although GDC-0449 has produced promising antitumor responses in patients with advanced basal cell carcinoma and medulloblastoma (47, 48), resistance to GDC-0449 has been reported in a patient with metastatic medulloblastoma who was initially highly responsive to GDC-0449 (49, 50). Gene sequencing of a recurrent, drug-resistant tumor from this patient has identified a SMO missense mutation, D473H, which decreased the binding affinity of GDC-0449 by 100-fold. Other mutations of human or murine SMO that render resistance to GDC-0449 have also been reported. In addition, other putative mechanisms of SMO-inhibitor resistance have also been identified, including *GLI2* and *Cyclin D1* (*CCND1*) amplification, and activation of the

PI3K-AKT signaling pathway (50). The resistance to SMO inhibitors highlights the therapeutic need to target downstream effectors to maintain robust on-target responses.

In a cell-based screen of GLI-mediated transcription, the small molecule GANT61 was identified as a specific inhibitor of GLI1 and GLI2 (51). The IC50 of GANT61 in suppressing the Gli-luciferase reporter activity in NIH 3T3 cells is approximately 5 μmol/L. GANT61 functions in the nucleus to suppress the DNA binding capacity of GLIs and inhibits both GLI1- and GLI2- mediated transcription. It has no influence on major but unrelated signaling pathways, including TNF signaling/ NFκB activation, glucocorticoid receptor gene transactivation, and the RAS-RAF-MEK-MAPK cascade. General and common cellular events, such as correct protein folding, nuclear transport, or basal transcriptional machinery assembly are not disturbed by GANT61. Moreover, GANT61 is inactive in several other screens for inhibitors of HGF/ Met, C/EBP$\alpha$ or HIF-1 (51). These studies collectively demonstrate a high selectivity of GANT61. GANT61 reduces proliferation and induces apoptosis in a GLI-specific fashion in prostate cancer (51), colon carcinoma (52, 53), oral squamous cell carcinoma (45), pancreatic cancer (54), neuroblastoma (55), and chronic lymphocytic leukemia (56). Figure 4 shows the chemical structures of cyclopamine, GDC-0449 and GANT61.

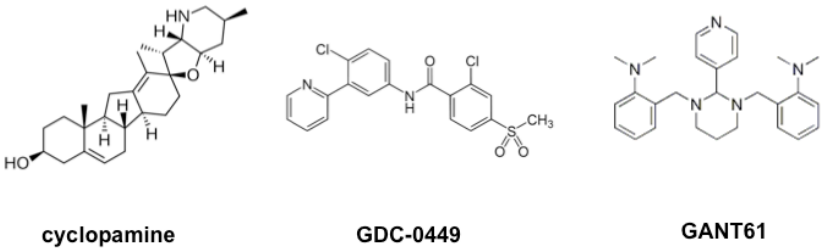


**Figure 4: Chemical structures of HH inhibitors**

# 2. Activation of HH-GLI signaling is associated with the classical subtype of human LSCC.

## *2.1 Materials and Methods*

### 2.1.1 RNAseq and microarray analysis of patient specimens

In collaboration with Dr. Vonn Walter and Dr. Neil Hayes at the University of North Carolina, we analyzed two independent patient cohorts: (1) RNA-seq data of 178 tumor samples from The Cancer Genome Atlas LSCC study (TCGA cohort) (20), and (2) microarray data of 56 LSCC samples collected at the University of North Carolina (UNC cohort) (19). RSEM values (57) for the (20) were converted to gene expression measurements by replacing all values equal to zero with the smallest non-zero value, taking a $\log_2$ transformation, and median centering by gene. Heatmaps of the gene expression values from (20) and (19) were produced with R 2.15.1 (58) and the gplots package. Hypotheses were subsequently tested: One-sided Wilcoxon Rank Sum tests were used to test the null hypothesis that the mean expression levels of *PTCH1*, *GLI1*, *GLI2*, *GLI3*, and *SUFU* are the same in the classical subtype as all other subtypes combined. For *PTCH1*, *GLI1*, and *GLI2*, the alternative hypothesis was that the expression levels are higher in the classical subtype, whereas for *GLI3* and *SUFU* the alternative hypothesis was that the expression levels are lower in the classical subtype. A Bonferroni adjustment was applied to correct for multiple comparisons.

Two-sided Wilcoxon Rank Sum tests were used to test the null hypothesis that *GLI1* and *GLI2* expression values were equal in the TCGA and UNC cohorts. Spearman

correlation coefficients were computed based on the uncentered expression values of *GLI1*, *GLI2*, *TP63, PIK3CA*, and *SOX2* in both the TCGA and UNC cohorts. The resulting unadjusted *p* values were used to assess the significance of these associations (Table 2).

## *2.2 Results*

### 2.2.1 Activation of HH-GLI signaling is associated with the classical subtype in both TCGA and UNC cohorts.

In collaboration with Dr. Vonn Walter and Dr. Neil Hayes, we queried the RNA expression data of 178 patient samples from the Cancer Genome Atlas (TCGA) LSCC study to ascertain whether HH signaling is upregulated in a particular subset of LSCC patients. As Figure 5 demonstrates, the expression of HH target genes (*PTCH1*, *GLI1*, *GLI2*) was significantly higher, while expression of negative regulators (*GLI3*, *SUFU*) was substantially lower in the classical subtype in comparison to the other subtypes. One-sided Wilcoxon Rank Sum Test confirmed these observations (Table 1) even after applying a Bonferroni adjustment for multiple comparisons. Similar expression patterns were seen in an independent cohort of 56 LSCC samples collected at the University of North Carolina (UNC cohort) (Figure 6).

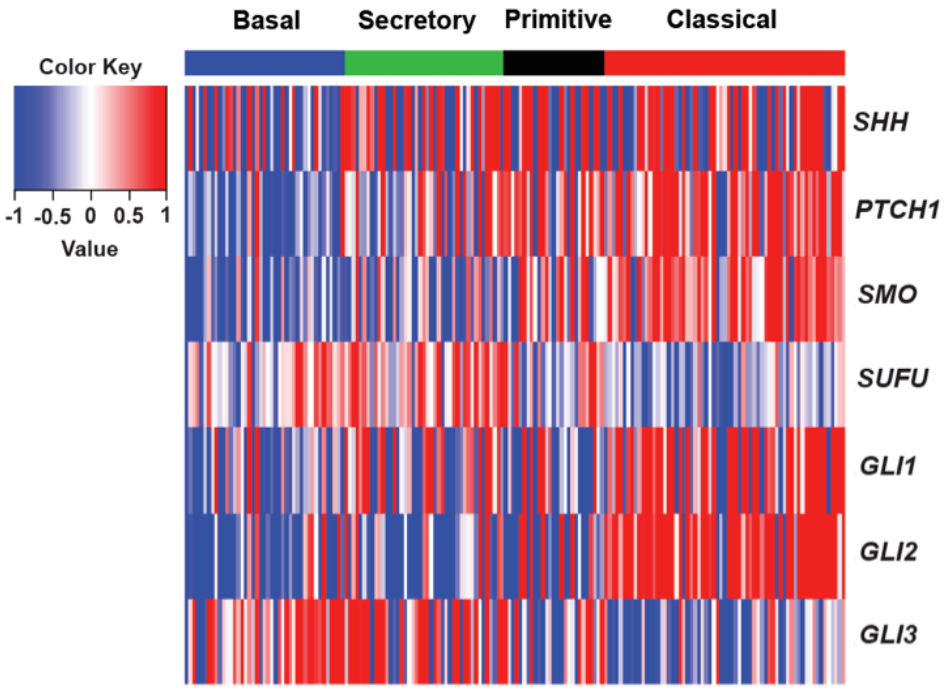


**Figure 5: HH activation pattern in the TCGA cohort**

Heatmap of HH signaling components in the TCGA cohort. Tumor samples are displayed as columns, grouped by gene expression subtypes. Selected HH genes are rows. Displayed genes of HH pathway except *SHH*, showed highly significant association with gene expression subtype ($p$<0.001) (Table 1).

**Table 1: Results of hypothesis tests used to compare expression values of HH genes in LSCC subtypes of the TCGA cohort**

| Gene | Alternative Hypothesis | Unadjusted p-value | Adjusted p-value |
|---|---|---|---|
| *PTCH1* | Greater in classical | 1.81e-7 | 9.07e-7 |
| *GLI1* | Greater in classical | 7.58e-8 | 3.79e-7 |
| *GLI2* | Greater in classical | 4.99e-16 | 2.49e-15 |
| *GLI3* | Less in classical | 1.20e-7 | 5.98e-7 |
| *SUFU* | Less in classical | 4.15e-10 | 2.08e-9 |

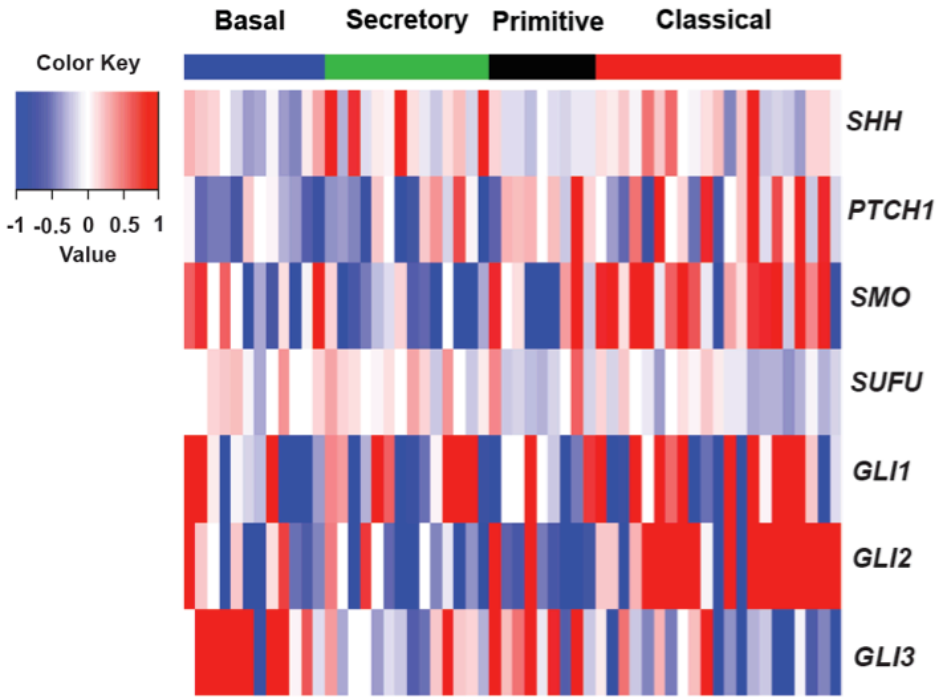


**Figure 6: HH activation pattern in the UNC cohort**

Heatmap of HH signaling components in the UNC cohort. Tumor samples are displayed as columns, grouped by gene expression subtypes. Selected HH genes are rows.

### 2.2.2 *GLI2* mRNA level is significantly higher than *GLI1*.

As shown in Figure 7, *GLI2* mRNA level was significantly higher than *GLI1* in both TCGA cohort ($p$=4.2×10$^{-5}$) and UNC cohort ($p$=0.016). Samples with high *GLI2* expression were mainly found in the classical subtype although occasionally in other subtypes (Figure 8). We defined the 75$^{th}$ percentile of all *GLI2* expression values in a given cohort as the threshold for high *GLI2*. In the TCGA cohort, 55% of all classical

subtype samples exhibit high *GLI2* expression. Only 9 of 45 samples with high level of *GLI2* lie outside the classical subtype. In the UNC cohort, 52% of all samples in the classical subtype exhibit high *GLI2* expression. Only 3 of 14 samples with high level of *GLI2* lie outside the classical subtype. These samples with high *GLI2* expression represent tumors with hyperactive HH signaling.

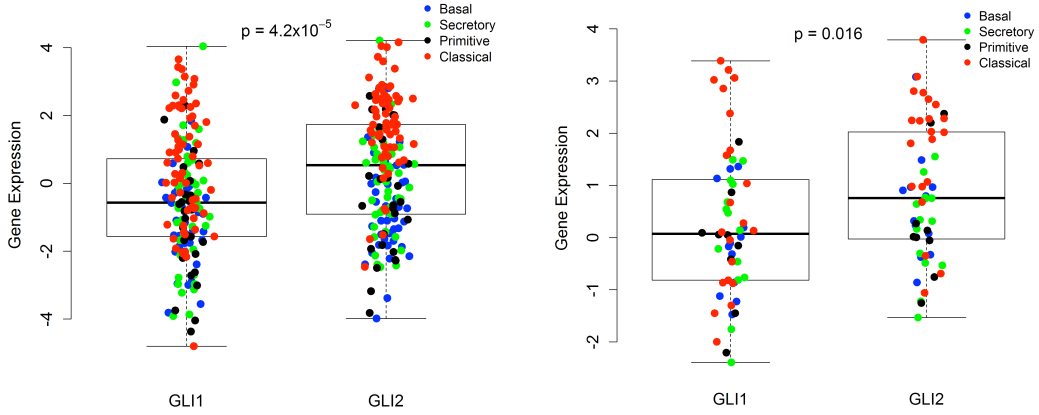


**Figure 7: Comparison of mRNA levels of *GLI1* and *GLI2***

Left: TCGA cohort. Right: UNC cohort. Gene expression values of individual patients are colored according to the subtypes.

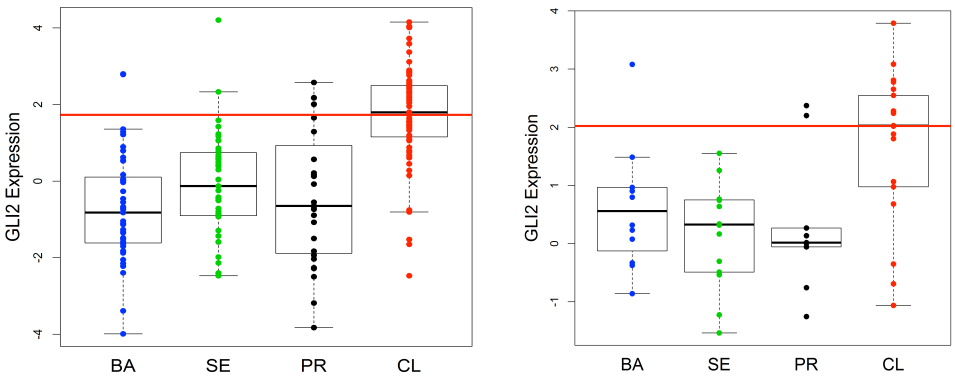


**Figure 8: Distribution of high *GLI2* samples in patient cohorts**

Left: TCGA cohort; Right: UNC cohort. Gene expression values are plotted according to subtypes, and the 75$^{th}$ percentile of all *GLI2* expression is shown as a horizontal red line.

### 2.2.3 *GLI2* is positively associated with the classical subtype markers.

In both cohorts, we observed strong positive correlations between *GLI2* and the prominent markers for the classical subtype on chromosome 3q: *SOX2* (Figure 9), *TP63* (Figure 10) and *PIK3CA* (Figure 11). However, *GLI1* was only associated with classical chr3q genes in the TCGA cohort (Figure 12), suggesting that *GLI2* is highly likely to be the major signaling transducer in LSCC. Spearman correlation coefficients between *GLI2*/ *GLI1* and the classical subtype markers with corresponding *p* values were summarized in Table 2.

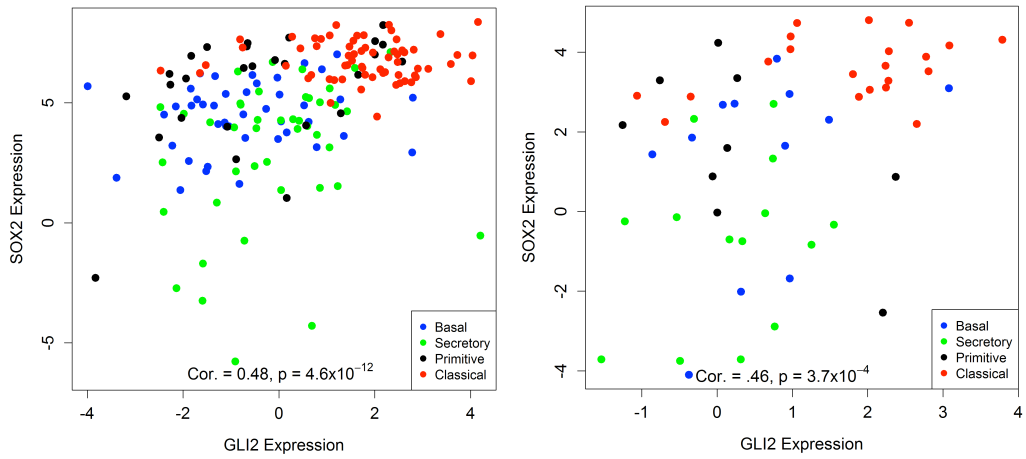


**Figure 9: Scatterplots of expression measurements between *GLI2* and *SOX2***

Left: TCGA cohort. Right: UNC cohort.

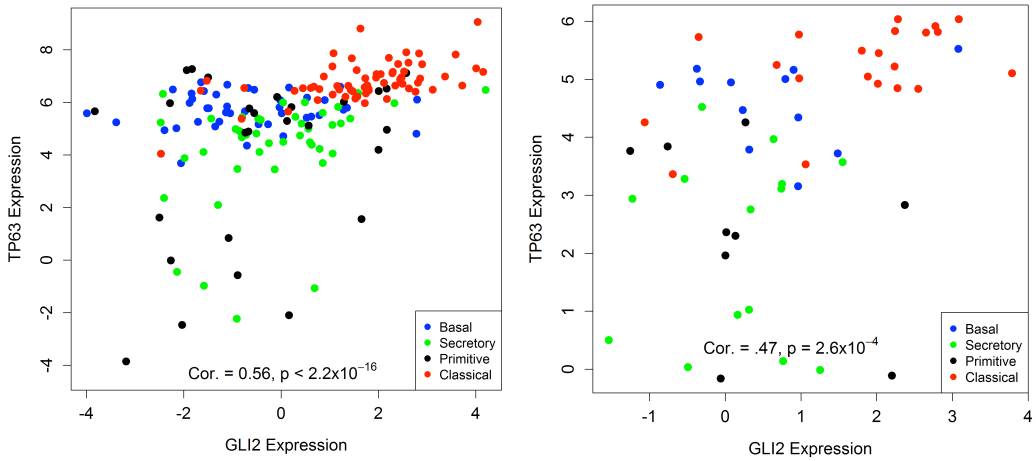


**Figure 10: Scatterplots of expression measurements between *GLI2* and *TP63***

Left: TCGA cohort. Right: UNC cohort.

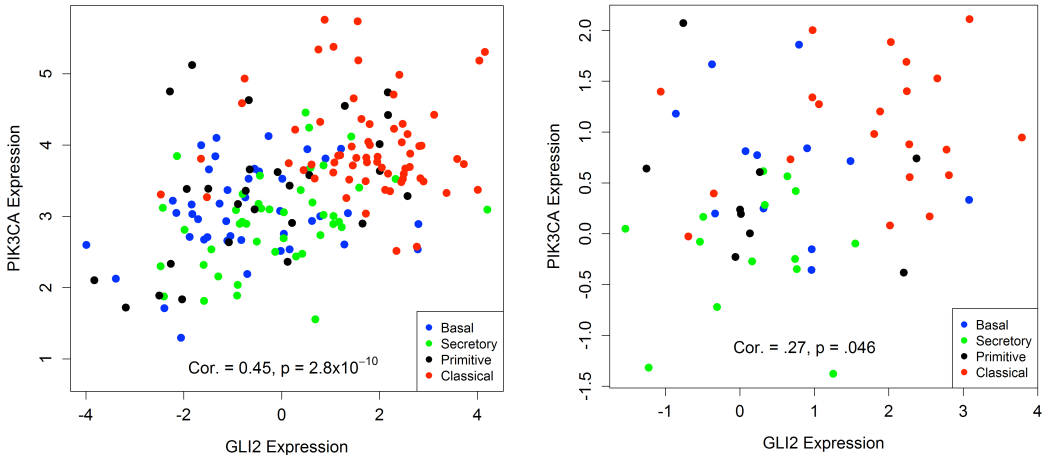


**Figure 11: Scatterplots of expression measurements between *GLI2* and *PIK3CA***

Left: TCGA cohort. Right: UNC cohort.

**Table 2: Spearman correlation coefficients and *p* values between *GLI2*/ *GLI1* and the classical subtype markers**

| Gene Name | | TCGA Cohort | | UNC Cohort | |
|---|---|---|---|---|---|
| | | Spearman Correlation Coefficient | *p* value | Spearman Correlation Coefficient | *p* value |
| *GLI2* | *SOX2* | 0.48 | $<4.6\times10^{-12}$ | 0.46 | $3.7\times10^{-4}$ |
| *GLI2* | *TP63* | 0.56 | $<2.2\times10^{-16}$ | 0.47 | $2.6\times10^{-4}$ |
| *GLI2* | *PIK3CA* | 0.45 | $2.6\times10^{-10}$ | 0.27 | 0.046 |
| *GLI1* | *SOX2* | 0.41 | $1.9\times10^{-8}$ | Not significant | |
| *GLI1* | *TP63* | 0.33 | $8.2\times10^{-6}$ | Not significant | |
| *GLI1* | *PIK3CA* | 0.31 | $2.1\times10^{-5}$ | Not significant | |

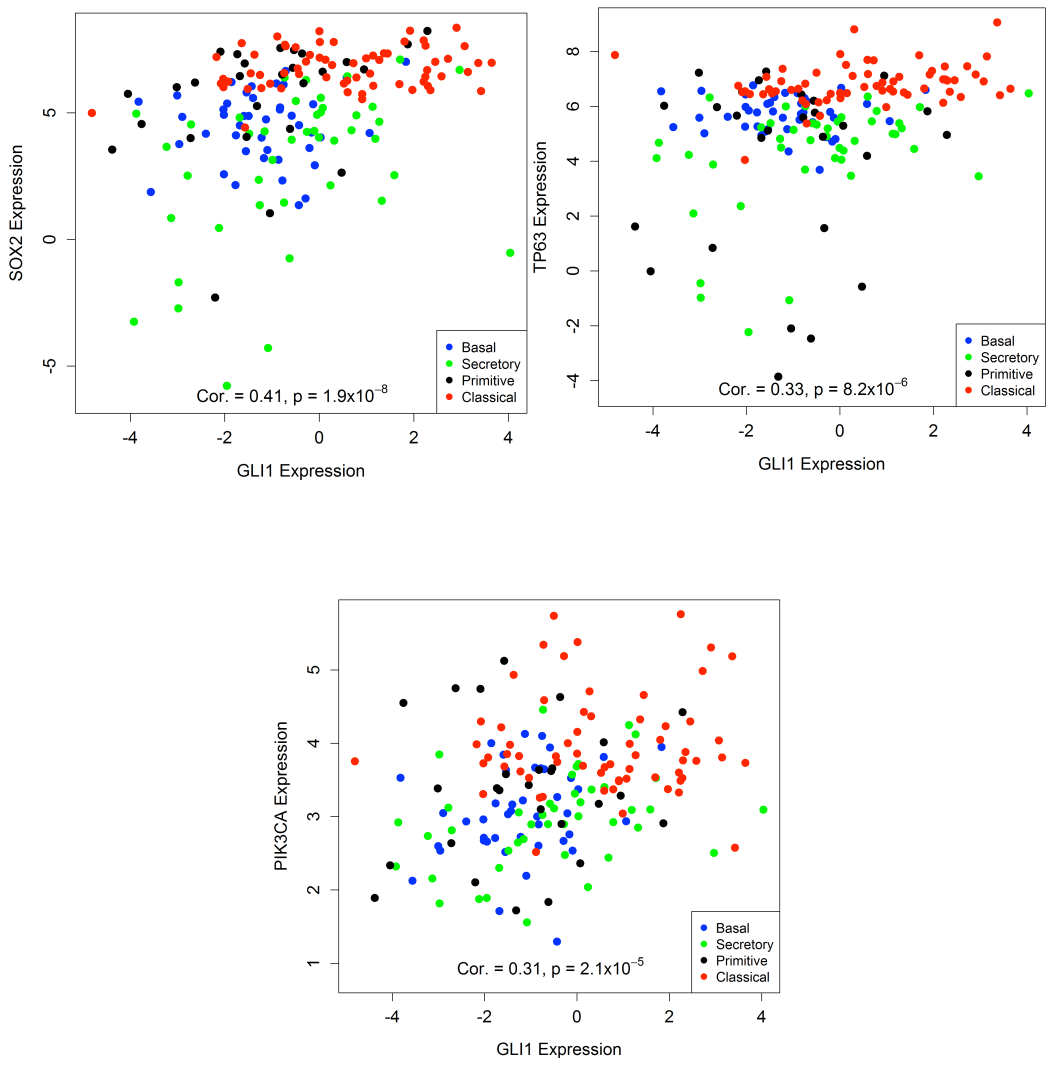


**Figure 12: Scatterplots of expression measurements of *GLI1* and classical subtype markers in the TCGA cohort**

*GLI1* is only correlated with *SOX2* (upper left), *TP63* (upper right), and *PIK3CA* (bottom) in the TCGA cohort.

## 2.3 Summary

LSCC has long been treated as a single disease due to the limited knowledge of the oncogenic drivers and tumor heterogeneity. The recent discovery of mRNA expression signatures has classified LSCC into four distinct subtypes with different biological features and survival outcomes. However, the clinical application of this molecular classification has not been evaluated. Previous IHC studies in patient specimens have reported overexpression of HH-GLI signaling molecules in a portion of LSCC samples, but failed to define this patient subset on a molecular basis. In our studies, we confirm the activation of HH-GLI pathway in a subset of LSCC patients. Notably, hyperactive HH-GLI signaling is associated with the classical subtype (≈36% of LSCC). *GLI2* mRNA level is significantly higher than *GLI1*, which suggests that GLI2 is the major signal transducer in LSCC. Due to the importance of GLI2 in HH signaling mediation, we consider high GLI2 expression as the criteria of defining tumors with hyperactive HH pathway. When taking the 75$^{th}$ percentile of all *GLI2* expression values in a given cohort as the threshold for high *GLI2*, 25% of total LSCC samples exhibit high expression of *GLI2*. This percentage is consistent with previous report in IHC studies, which show high activation of HH signaling in 27% of all LSCC specimens. Approximately 55% of the classical subtype samples display high expression of *GLI2*, while samples with high level of *GLI2* are occasionally found in other subtypes. We also observe strong positive correlations between *GLI2* and the classical subtype markers

(*SOX2*, *TP63* and *PIK3CA*). These findings revealed aberrant activation of HH signaling in the classical subtype, featuring a consistently high expression of *GLI2* and indicating a potentially critical role of GLI2 in the classical subtype.

# 3. HH-GLI signaling components are expressed in human LSCC cell lines.

## *3.1 Materials and Methods*

### 3.1.1 Cell culture and reagents

NCI-H520, NCI-H2170, NCI-H226 and SK-MES-1 cells were obtained from ATCC. Cell lines were routinely verified by morphology and growth characteristics, and verified biannually to be mycoplasma-free. NCI-H520, NCI-H2170 and NCI-H226 cells were maintained in the RPMI 1640 medium containing 10% fetal bovine serum (FBS). SK-MES-1 cells were maintained in MEM medium containing 10% FBS, 0.1 mM non-essential amino acids, 1.0 mM sodium pyruvate.

### 3.1.2 RNA isolation and Real-time PCR

Total RNA was isolated using the Qiagen RNeasy Mini Kit, treated with DNase I (Invitrogen) and converted to cDNA using iScript cDNA Synthesis Kit (BIO-RAD). Real-time PCR was performed using TaqMan Gene Expression Master Mix on an Eppendorf Mastercycler, and raw data were analyzed by Realplex software. TaqMan probes for *SHH*, *PTCH1*, *SMO*, *GLI1*, *GLI2*, and *GAPDH* were purchased from Applied Biosystems.

### 3.1.3 Western analysis

Total cellular lysates were prepared by using RIPA buffer (Sigma) with addition of protease inhibitor cocktail (Sigma) and PhosSTOP (Roche). Protein concentrations were determined by Micro BCA Protein Assay Kit (Thermo Scientific). Proteins were

separated on the NuPAGE 4-12% Bis-Tris Gel (Life Technologies) and transferred using Invitrolon PVDF Filter Paper Sandwich. Membranes were blocked with 5% nonfat dry milk in Tris-buffered saline with 0.1% Tween 20 (0.1% TBST) for 1 hour in room temperature, then incubated with primary antibody overnight at 4°C. Membranes were subsequently washed with 0.1%TBST and incubated with the secondary antibody for 1 hour at room temperature. Western Lightning- ECL (PerkinElmer) was used to develop the membranes. Antibodies: SHH, PTCH, SMO (Santa Cruz); GLI1 (Novus Biologicals); GLI2, GAPDH (Abcam).

### 3.1.4 Subtype prediction and validation in LSCC cell lines

Gene expression data from 20 LSCC cell lines was obtained from the Cancer Cell Line Encyclopedia (CCLE) (59). After median centering the expression values by gene, the centroid classifier from (19) was used to predict expression subtypes for each line by finding the nearest centroid using a distance metric equal to one minus the Pearson correlation coefficient. Gene expression heatmaps were then produced using R2.15.1 (58) and the gplots package.

## *3.2 Results*

### 3.2.1 HH-GLI signaling components are present in human LSCC cell lines.

The difficulty of growing human LSCC cells *in vitro* limits available primary cancer cells to test. Therefore, we chose the four most widely used human LSCC cell lines to analyze active HH signaling: NCI-H520 and NCI-H2170, derived from primary

tumors; and NCI-H226 and SK-MES-1, derived from metastatic pleural effusions. By real-time PCR (Figure 13A) and Western blots (Figure 13B), high levels of SHH were detected only in NCI-H520, whereas PTCH1 and SMO were expressed universally across all four lines. Neither GLI1 nor GLI2 was detected in NCI-H2170. In the remaining three lines, GLI1 was expressed at a low level, whereas high levels of GLI2 were consistently detected at both the mRNA and protein level.

### 3.2.2 NCI-H520 and NCI-H2170 represent classical LSCC, while NCI-H226 and SK-MES-1 represent secretory LSCC.

In order to ascertain whether these cell lines represent different human primary LSCC subtypes by mRNA expression, gene expression profiles from CCLE (59) were analyzed. NCI-H520 and NCI-H2170 were predicted to be classical subtype, and NCI-H226 and SK-MES-1 as secretory subtype. Gene expression of the subtypes between the cell lines and patient tumors is consistent over the validation gene set (Figure 14).

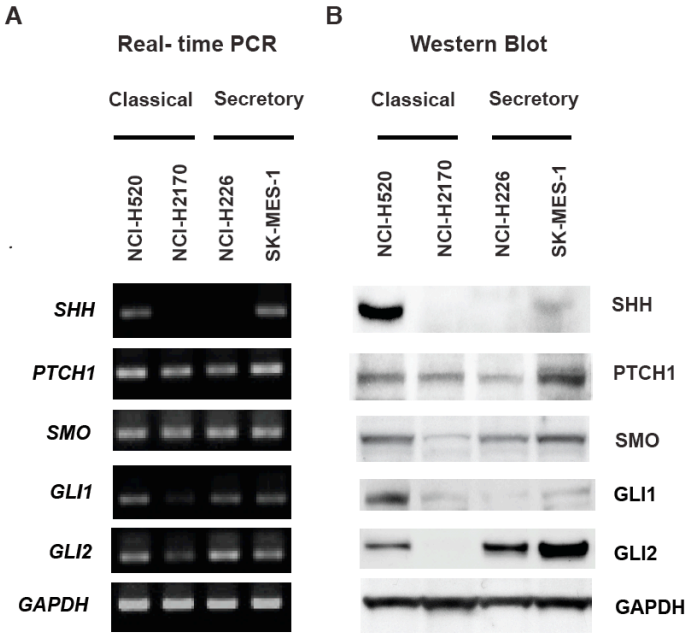


**Figure 13: HH signaling components are expressed in LSCC cell lines**

A. Real-time PCR for indicated genes, with *GAPDH* as the quantitative control.

B. Western Blot for the SHH-GLI pathway components, with GAPDH as the loading control. Classical subtype: NCI-H520 and NCI-H2170; Secretory subtype: NCI-H226 and SK-MES-1.

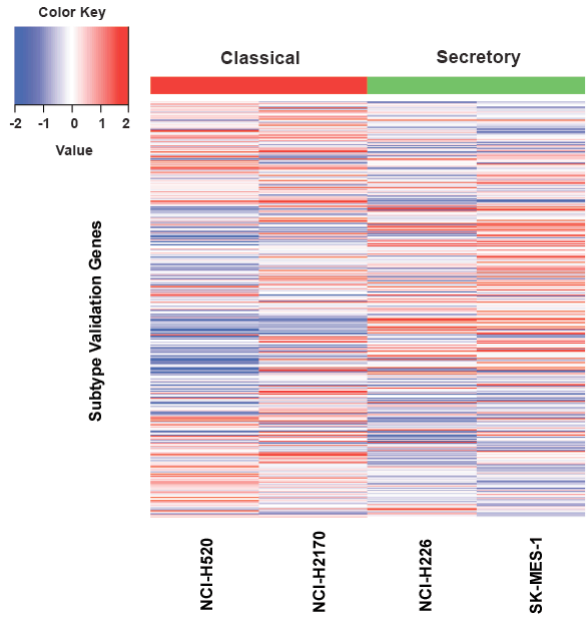


**Figure 14: Heatmap of subtype validation gene expression for LSCC cell lines**

Classical subtype: NCI-H520 and NCI-H2170; Secretory subtype: NCI-H226 and SK-MES-1. Subtype prediction was based on the expression subtype classifier genes as described by Wilkerson et al. (19). Expression patterns for cell lines predicted to be in the classical or secretory subtypes are similar to those seen in Figure 2 of Wilkerson et al.

## *3.3 Summary*

We observe the expression of HH-GLI signaling molecules in the four most widely used human LSCC cell lines, which provide valuable resources for further study. These cell lines represent the classical and secretory subtypes respectively as observed in primary human LSCC. When the classical subtype contains the highest percentage of high *GLI2* samples, a few samples show low level of *GLI2* comparable to the majority of

the other three subtypes. Although both predicted as the classical subtype, NCI-H520 and NCI-H2170 represent two different levels of HH activation. NCI-H226 and SK-MES-1 may represent individual samples in the secretory subtype that display high expression of *GLI2*.

# 4. SMO plays a minor role in HH-GLI signaling mediation and survival in LSCC cell lines.

## *4.1 Materials and Methods*

### 4.1.1 Lentiviral production and transduction

Lentiviral shRNA clones (Sigma Mission RNAi) targeting SMO and the non-targeting control (SHC002) were purchased from Sigma-Aldrich. 293T cells were plated in 10-cm plates 24 hours prior to transfection in DMEM medium containing 10% fetal bovine serum (FBS) without antibiotics. 5 μg shRNA plasmid, 4 μg psPAX2 and 1 μg pCI-VSVG packaging vectors (Addgene) were co-transfected into 293T cells using Lipofectamine 2000 Reagent (Invitrogen). Viral supernatants were collected, centrifuged and filtered with 0.45 μm PES Sterile Syringe Filter. Target cells were plated and incubated at 37°C, 5% $CO_2$ overnight, and changed to medium containing lentivirus and 8 μg/mL polybrene. Control plates were incubated with medium containing 8 μg/mL polybrene. Cells were changed to fresh culture medium 24 hours after infection. Puromycin selection (5 μg/ml) was started 48 hours post infection and continued for 4~5 days until no viable cells were observed in control plates. Once decreased expression of the targeted gene was confirmed, cells were used for subsequent experiments. Stable expression of non-targeting control or SMO shRNAs was ensured by culturing cells in the presence of puromycin. Sequences of shRNA constructs are provided as below:

SMO sh1 (5'- CCGGCCTGATGGACACAGAACTCATCTCGAGATGAGTTCTG TGTCCATCAGGTTTTT-3')

SMO sh2 (5′- CCGGCATCTTTGTCATCGTGTACTACTCGAGTAGTACACGA TGACAAAGATGTTTTT-3′)

SMO sh3 (5′- CCGGGTGGAGAAGATCAACCTGTTTCTCGAGAAACAGGTTG ATCTTCTCCACTTTTT-3′)

### 4.1.2 RNA isolation and Real-time PCR

Total RNA was isolated using the Qiagen RNeasy Mini Kit, treated with DNase I (Invitrogen) and converted to cDNA using iScript cDNA Synthesis Kit (BIO-RAD). Real-time PCR was performed using TaqMan Gene Expression Master Mix on an Eppendorf Mastercycler, and raw data were analyzed by Realplex software. TaqMan probes for *PTCH1*, *SMO*, *GLI2*, *HHIP1*, and *GAPDH* were purchased from Applied Biosystems.

### 4.1.3 Assessment of cell viability and caspase 3/7 activity

In GDC-0449 treatment, cells were seeded in 96-well clear-bottom white plates (Corning Costar) at a density of 10,000 cells per well and incubated with complete medium overnight at 37°C, 5% $CO_2$. The following day, cells were changed into 0.5% FBS-containing medium with either DMSO control or GDC-0449 (Chemietek) at designated concentrations (0.1% final DMSO concentration) as triplicates and treated for 96 hours. At the end of treatment, cell viability and caspase 3/7 activity were determined by using ApoLive-Glo Multiplex Assay (Promega) according to the manufacturer's instructions. Briefly, viability reagent was added into all wells and gently mixed. After 1.5-hour incubation at 37°C, fluorescence was measured at the wavelength set $355_{EX}$/

$520_{EM}$ by a FLUOstar Omega Microplate reader. Later, Caspase-Glo® 3/7 Reagent was added to all wells and gently mixed. Luminescence was measured after 1-hour incubation at room temperature. The reading of blank control was subtracted from readings of other wells as the background in the data analysis. In shRNA experiments, after evaluation of knockdown efficiency, cells were tested for viability and caspase 3/7 activity. Cells were seeded in 96-well clear-bottom white plates at a density of 10,000 cells per well and incubated with complete medium containing 5 μg/ml puromycin at 37°C, 5% $CO_2$. Cell viability and caspase 3/7 activity were accessed as described above.

## *4.2 Results*

### 4.2.1 shRNA knockdown of SMO produces minor effects on LSCC survival.

The universal expression and the ability to target SMO with multiple available inhibitors prompted us to investigate the importance of SMO in LSCC cells. As demonstrated in Figure 15, lentiviral-mediated expression of two independent SMO shRNA constructs successfully reduced the SMO mRNA level by 70~90% in four cell lines in comparison to the non-targeting control (ShNT). However, only minor effects on cell viability and apoptosis were observed in these cells (Figure 16A, B), indicating a dispensable role of SMO in regulation of cell survival and cell death in LSCC cells.

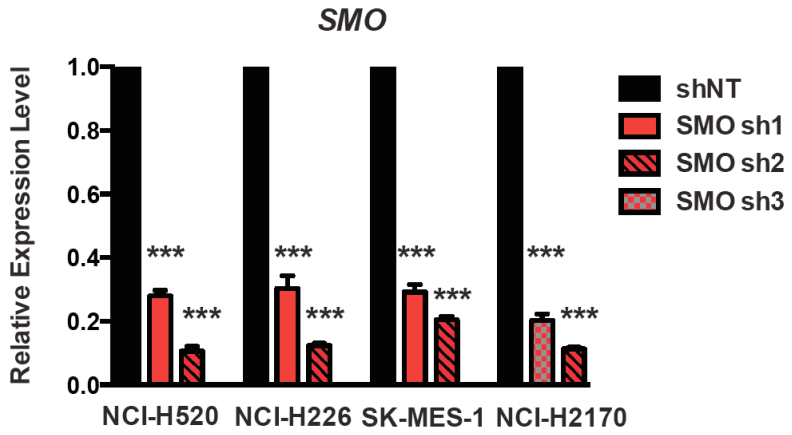


**Figure 15: shRNA knockdown of SMO in LSCC cells**

Change of *GAPDH*-normalized *SMO* mRNA level by real-time PCR following lentiviral shRNA knockdown. Non-targeting shRNA control (shNT) or 2 independent shRNAs (SMO sh1, 2, 3) targeting SMO were used in each cell line. Data were normalized to shNT control and represent the mean ± SD of 3 independent experiments. Data were analyzed by two-tailed t test, ***: $p<0.001$.

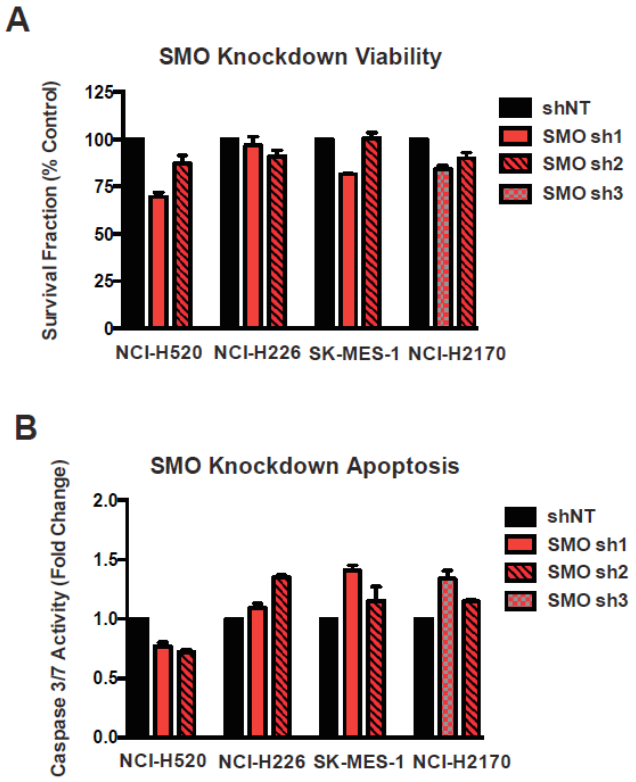


**Figure 16: Measurements of cell viability and apoptosis after SMO knockdown**

Viability (A) and apoptosis (B) were evaluated in cells after SMO knockdown by using ApoLive-Glo Multiplex Assay (Promega). Data were normalized to shNT control and represent the mean ± SD of 3 independent experiments.

### 4.2.2 SMO deletion produces minimal influence on downstream HH-GLI signaling in LSCC cells.

We next examined the expression level of HH targets downstream of SMO. As shown in Figure 17A, SMO knockdown caused a moderate decrease of *PTCH1* mRNA in NCI-H520 and NCI-H226, whereas no reduction of *PTCH1* mRNA was seen in NCI-

H226 and SK-MES-1. No significant reduction of *HHIP* mRNA in any of four cell lines (Figure 17B). These data suggest a minimal role for SMO in regulating LSCC survival via the canonical HH pathway. Interestingly, loss of SMO did not reduce *GLI2* mRNA level in three GLI-positive cell lines. Instead, we noted a slight increase of *GLI2* mRNA (Figure 17C), which may be caused by compensatory upregulation of *GLI2* by other SMO-independent mechanisms.

### 4.2.3 SMO inhibitor GDC-0449 shows limited cytotoxicity in LSCC cells.

Recently, SMO inhibitors have demonstrated promising anti-tumor activity in clinical treatments of medulloblastoma and basal cell carcinoma. To investigate the feasibility of pharmacologically targeting SMO in LSCC, we studied the therapeutic potential of a clinically available SMO inhibitor, GDC-0449. To maintain physiologic relevance and minimize off-target toxicity, we assessed the efficacy of GDC-0449 in four LSCC cell lines at the concentrations of 2.5, 5 and 10 μmol/L. Cells were treated in triplicate with either DMSO control or GDC-0449 for 96 hours, and then assayed for viability and caspase 3/7 activation.

As shown in Figure 18A, treatment of GDC-0449 in NCI-H520 led to 20% reduction of viable cells at 5 μmol/L, and approximate 50% reduction at 10 μmol/L. NCI-H226 only showed a moderate 15% decrease of viable cells at 10 μmol/L. No significant growth inhibition was observed in SK-MES-1 and NCI-H2170 cells treated with GDC-0449. Consistently, GDC-0449 induced limited increase of caspase 3/7 activities in NCI-

H520 (1.3 fold increase at 5 μmol/L and 1.6 fold increase at 10 μmol/L) and NCI-H226 (1.6 fold increase at 10 μmol/L) (Figure 18B). Despite the universal expression of SMO, GDC-0449 showed limited growth inhibition and apoptosis induction in LSCC cells, which is consistent with our observations in SMO knockdown experiments.

### 4.2.4 SMO suppression by GDC-0449 shows limited impacts on downstream HH-GLI signaling in LSCC cells.

In agreement with the limited growth inhibition, GDC-0449 only caused modest reduction of *PTCH1* mRNA in NCI-H226 cells, which suggested that GDC-0449 failed to suppress downstream signaling in these cells (Figure 19A). Among three GLI-positive cell lines, GDC-0449 led to slight decrease of *GLI2* mRNA only in NCI-H226 and SK-MES-1 (Figure 19B). This finding again demonstrated that GDC-0449 was unable to block the HH-GLI signaling downstream of SMO, indicating a minimal role of SMO in mediating HH-GLI signaling in LSCC.

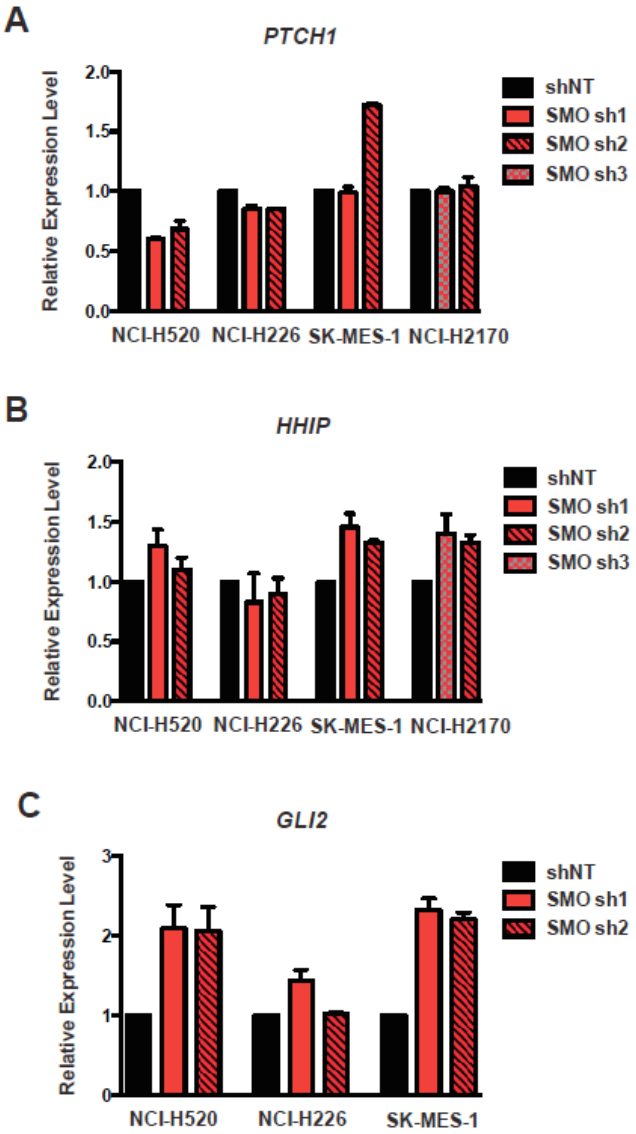


**Figure 17: Expression of HH downstream target genes after SMO knockdown**

Real-time PCR analysis showed the *GAPDH*-normalized mRNA level of *PTCH1* (A), *HHIP* (B) and *GLI2* (C) after SMO knockdown. Data were normalized to shNT control and represent the mean ± SD of 3 independent experiments.

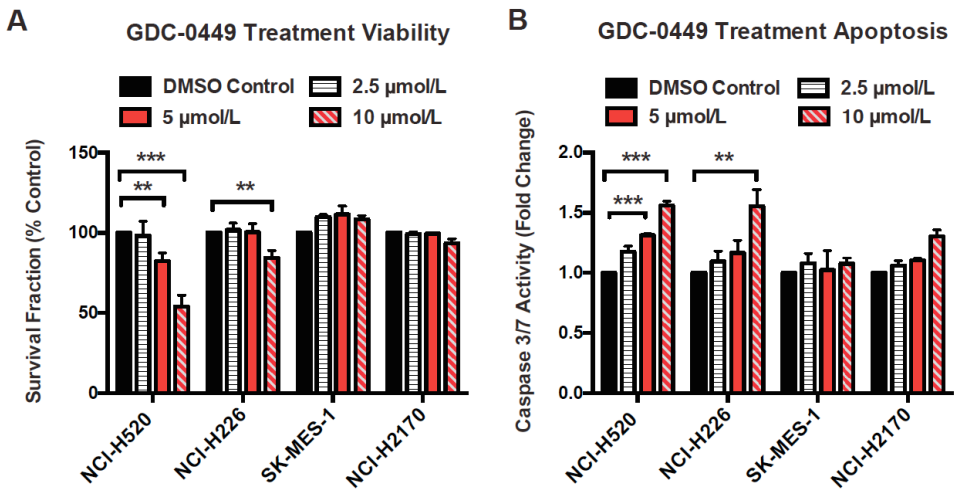


**Figure 18: GDC-0449 treatment in LSCC cells**

96-hour treatment of GDC-0449 generated limited growth inhibition (A) and apoptosis (B). Only moderate cytotoxicity was observed in NCI-H520 and NCI-H226 cells at 10 µmol/L. Data were normalized to DMSO control and represent the mean ± SD of 3 independent experiments. (Two-tailed t test, **: $p<0.01$; ***: $p<0.001$)

## *4.3 Summary*

The universal expression of SMO and its importance in HH signaling transduction prompted us to evaluate the effects of SMO inhibition in LSCC cells, because there are multiple clinically-available SMO antagonists. However, neither genetic nor pharmacological inhibition of SMO produces satisfying growth inhibition and apoptosis induction in four LSCC cell lines. Further analysis shows that suppression of SMO has limited impacts on downstream HH signaling, evident by modest changes of expression levels of HH target genes. These findings collectively demonstrate a

dispensable role of SMO in regulation of LSCC cell survival via mediating HH-GLI signaling. In fact, multiple studies have documented SMO-independent regulation of HH-GLI signaling via non-canonical pathways, including SUFU loss-of-function mutations, GLI gain-of-function mutations, and GLI activation by PI3K/AKT or RAS/MEK signaling pathways (21, 60). Interestingly, amplification of *GLI2* has been proposed as putative mechanism responsible for resistance to SMO inhibitors (50). Since we have observed high expression of GLI2 in human primary LSCC, as well as in LSCC cell lines, we continued to explore the role of GLI2 in LSCC.

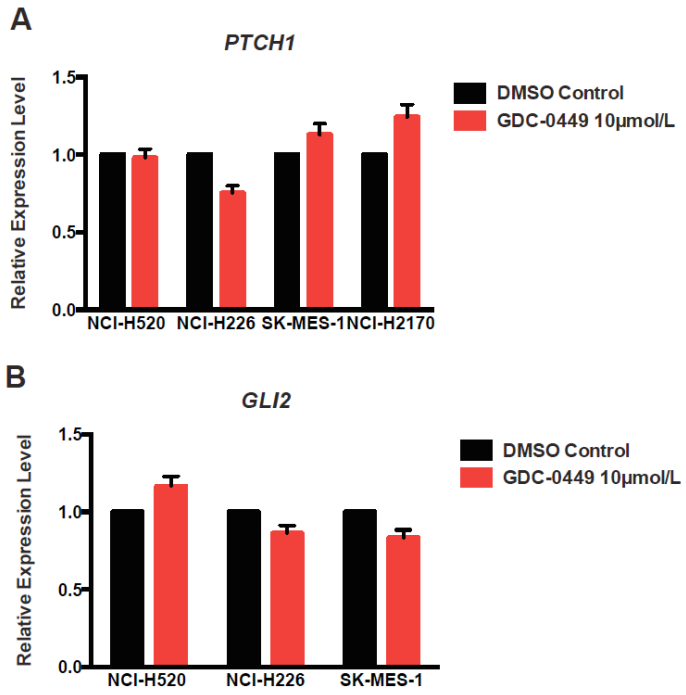


**Figure 19: Expression of HH target genes after GDC-0449 treatment**

Real-time PCR showed the mRNA level of *PTCH1* (A) and *GLI2* (B) in LSCC cells treated with DMSO or 10 μmol/L GDC-0449 for 96 hours. Gene expressions were normalized to endogenous *GAPDH* in each cell line. Data represent the mean ± SD of 3 independent experiments.

# 5. GLI2 plays an important role in regulating LSCC cell survival and apoptosis.

## *5.1 Materials and Methods*

### 5.1.1 Lentiviral production and transduction

Lentiviral shRNA clones (Sigma Mission RNAi) targeting GLI2 and the non-targeting control (SHC002) were purchased from Sigma-Aldrich. 293T cells were plated in 10-cm plates 24 hours prior to transfection in DMEM medium containing 10% fetal bovine serum (FBS) without antibiotics. 5 μg shRNA plasmid, 4 μg psPAX2 and 1 μg pCI-VSVG packaging vectors (Addgene) were co-transfected into 293T cells using Lipofectamine 2000 Reagent (Invitrogen). Viral supernatants were collected, centrifuged and filtered with 0.45 μm PES Sterile Syringe Filter. Target cells were plated and incubated at 37°C, 5% $CO_2$ overnight, and changed to medium containing lentivirus and 8 μg/mL polybrene. Control plates were incubated with medium containing 8 μg/mL polybrene. Cells were changed to fresh culture medium 24 hours after infection. Puromycin selection (5 μg/ml) was started 48 hours post infection and continued for 4~5 days until no viable cells were observed in control plates. Once decreased expression of the targeted gene was confirmed, cells were used for subsequent experiments. Stable expression of non-targeting control or GLI2 shRNAs was ensured by culturing cells in the presence of puromycin. Sequences of shRNA constructs are provided as below:

GLI2 sh1 (5′- CCGGCCAACGAGAAACCCTACATCTCTCGAGAGATGTAGGGT TTCTCGTTGGTTTTTG-3′)

GLI2 sh2 (5′-CCGGCACTCAAGGATTCCTGCTCATCTCGAGATGAGCAGGAA TCCTTGAGTGTTTTTG-3′)

GLI2 sh3 (5′-CCGGGCTCTACTACTACGGCCAGATCTCGAGATCTGGCCGTA GTA GTAGAGCTTTTTG-3′)

### 5.1.2 Western analysis

Total cellular lysates were prepared by using RIPA buffer (Sigma) with protease inhibitor cocktail (Sigma) and PhosSTOP (Roche). Protein concentrations were determined by Micro BCA Protein Assay Kit (Thermo Scientific). Proteins were separated on the NuPAGE 4-12% Bis-Tris Gel (Life Technologies) and transferred using Invitrolon PVDF Filter Paper Sandwich. Membranes were blocked with 5% nonfat dry milk or 5% BSA in 0.1%TBST for 1 hour in room temperature, then incubated with primary antibody overnight at 4°C. They were subsequently washed with 0.1%TBST and incubated with the secondary antibody for 1 hour at room temperature. Western Lightning- ECL (PerkinElmer) was used to develop the membranes. Antibodies against GLI2 and GAPDH were purchased from Abcam, Cleaved Caspase-3 and Cleaved PARP from Cell Signaling Technology, and CCND1 from BD Biosciences.

### 5.1.3 RNA isolation and Real-time PCR

Total RNA was isolated using the Qiagen RNeasy Mini Kit, treated with DNase I (Invitrogen) and converted to cDNA using iScript cDNA Synthesis Kit (BIO-RAD). Real-time PCR was performed using TaqMan Gene Expression Master Mix on an Eppendorf

Mastercycler, and raw data were analyzed by Realplex software. TaqMan probes for *PTCH1*, *GLI2*, *HHIP1*, and *GAPDH* were purchased from Applied Biosystems.

### 5.1.4 Assessment of cell viability and caspase 3/7 activity

In GANT61 treatment, cells were seeded in 96-well clear-bottom white plates (Corning Costar) at a density of 10,000 cells per well and incubated with complete medium overnight at 37°C, 5% $CO_2$. The following day, cells were changed into 0.5% FBS-containing medium with either DMSO control or GANT61 (Sigma-Aldrich) at designated concentrations (0.1% final DMSO concentration) as triplicates and treated for 96 hours. At the end of treatment, cell viability and caspase 3/7 activity were determined by using ApoLive-Glo Multiplex Assay (Promega) according to the manufacturer's instructions. Briefly, viability reagent was added into all wells and gently mixed. After 1.5-hour incubation at 37°C, fluorescence was measured at the wavelength set $355_{EX}$/ $520_{EM}$ by a FLUOstar Omega Microplate reader. Later, Caspase-Glo® 3/7 Reagent was added to all wells and gently mixed. Luminescence was measured after 1-hour incubation at room temperature. The reading of blank control was subtracted from readings of other wells as the background in the data analysis. In shRNA experiments, after evaluation of knockdown efficiency, cells were tested for viability and caspase 3/7 activity. Cells were seeded in 96-well clear-bottom white plates at a density of 10,000 cells per well and incubated with complete medium containing 5 μg/ml puromycin at 37°C, 5% $CO_2$. Cell viability and caspase 3/7 activity were accessed as described above.

## *5.2 Results*

### 5.2.1 Targeting GLI2 with shRNAs inhibits LSCC cell growth and induces extensive apoptosis.

Since *GLI1* is hardly detectable and high level of *GLI2* is consistently expressed in three cell lines and across human LSCC tumors, we focused on *GLI2*. Independent lentiviral-based GLI2 shRNAs achieved satisfactory knockdown of GLI2 protein in all three GLI2-positive lines (Figure 20). Knockdown of GLI2 reduced the protein level of the GLI target Cyclin D1 (CCND1), which is a direct target of GLI2 that regulates cell cycle and promotes cell proliferation (Figure 20). Loss of GLI2 also induced extensive apoptosis, demonstrated by strong induction of cleaved caspase-3 and cleaved PARP (Figure 20). These molecular changes were consistent with the strong inhibition of cell proliferation and survival (Figure 21A), as well as extensive apoptosis evident by elevated caspase 3/7 activity (Figure 21B). These data collectively demonstrate an important role of GLI2 in regulating LSCC cell survival, raising the possibility that GLI2 is a therapeutic target in human LSCC.

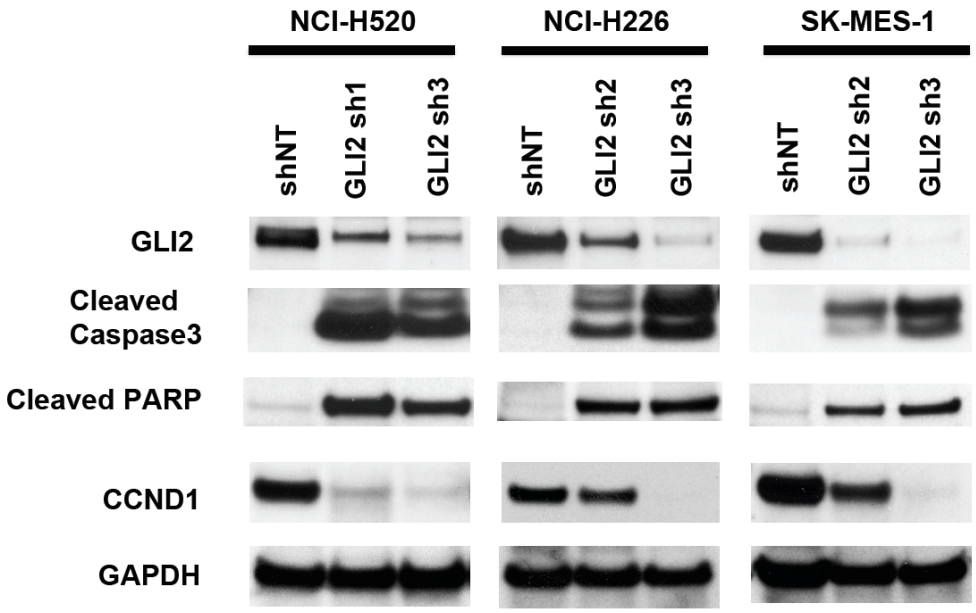


**Figure 20: shRNA knockdown of GLI2 in LSCC cells**

Western blots showing GLI2 knockdown by independent shRNAs (GLI2 sh1, 2, 3). GLI2 shRNAs significantly reduced GLI2 protein levels, in comparison to the shNT control. GLI2 knockdown also caused induction of cleaved caspase-3, cleaved PARP and reduction of CCND1. GAPDH was used as the loading control. A representative Western blot from 3 independent experiments is shown.

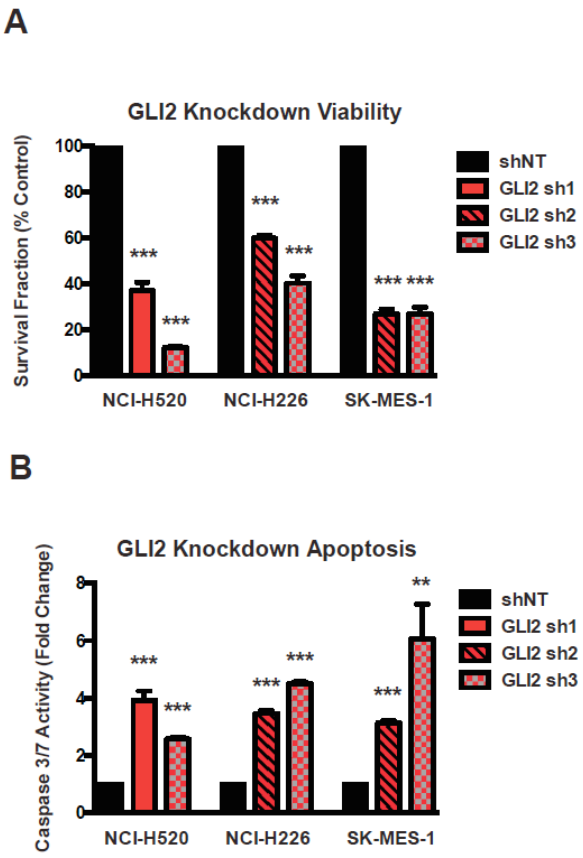


**Figure 21: Measurements of viability and apoptosis in LSCC cells after GLI2 knockdown**

Knockdown of GLI2 in LSCC cells significantly reduced proliferation (A) and induced apoptosis (B). Data were normalized to shNT control and represent the mean ± SD of 3 independent experiments. (Two-tailed t test, **: $p<0.01$; ***: $p<0.001$)

### 5.2.2 GLI inhibitor GANT61 leads to significant growth inhibition and apoptosis in LSCC cells.

In order to study the therapeutic potential of pharmacologically targeting GLI proteins in LSCC, we employed GANT61, a newly described small molecule that

selectively blocks both GLI1 and GLI2- mediated transcription. The originally reported IC50 of GNAT61 to reduce GLI-luciferase reporter activity is ≈5 μmol/L (51), and the commonly used concentration of GANT61 *in vitro* ranging from 5~30 μmol/L (52, 53). To maintain physiologic relevance and minimize off-target toxicity, we assessed the efficacy of GANT61 on four LSCC cell lines at the concentrations of 2.5, 5 and 10 μmol/L (Figure 22A). Cells were treated in triplicate with either DMSO control or GANT61 for 96 hours, and then assayed for viability and caspase 3/7 activation with Apolive-Glo (Promega), as described in Materials and Methods. The IC50 of growth inhibition in this assay for three GLI-positive cell lines was approximately 5 μmol/L. Both NCI-H520 and NCI-H226 showed a 55% reduction at 5 μmol/L and 90% reduction at 10 μmol/L in cell survival. SK-MES-1 displayed approximate 40% and 60% decrease in viability at 5 and 10 μmol/L, respectively. As expected, GANT61 exhibited little cytotoxicity in the GLI-negative cell line, NCI-H2170, in line with the high selectivity of this GLI inhibitor. Consistently, increased apoptosis was seen in GLI-positive cell lines at corresponding GANT61 concentrations: NCI-H520 (1.8~2.3 fold), NCI-H226 (2.8~4 fold) and SK-MES-1 (2.4~2.6 fold). No increased caspase 3/7 activity was detected in GLI-negative NCI-H2170 cells after GANT61 treatment (Figure 22B). In contrast to GDC-0449, GANT61 showed greater growth inhibition and apoptosis induction at equimolar concentrations at the same time point, demonstrating a higher efficacy than GDC-0449 in a dose-dependent manner in all GLI-positive cell lines. Our results suggest that targeting the HH signaling

pathway at the level of GLI proteins may be more effective than targeting either the ligand SHH or the receptor SMO in LSCC, potentially due to the existence of the ligand or receptor independent pathway activation as reported in previous studies.

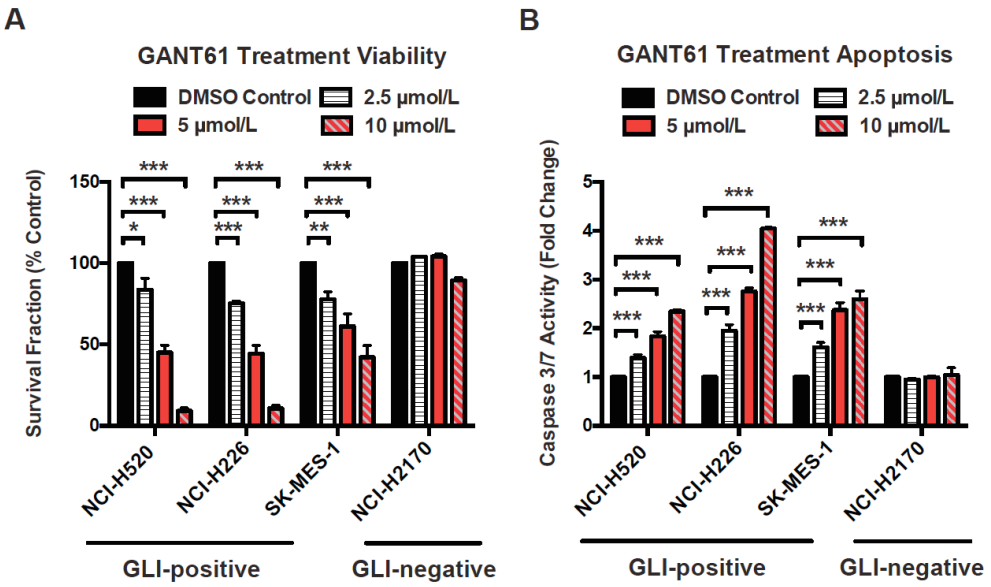


**Figure 22: GANT61 treatment in LSCC cells**

96-hour treatment of GANT61 significantly reduced cell survival (A) and induced extensive apoptosis (B) in all GLI-positive cell lines. GLI-negative NCI-H2170 was not affected by GANT61. Data were normalized to DMSO control and represent the mean ± SD of 3 independent experiments. (Two-tailed t test, *: $p<0.05$; **: $p<0.01$; ***: $p<0.001$)

### 5.2.3 GANT61 treatment reduces the expression of HH-GLI target genes.

The influence of GANT61 on the expression of HH target genes was subsequently determined in GLI-positive cell lines for up to 96 hours after treatment. Real-time PCR analysis showed that 10 μmol/L GANT61 treatment resulted in moderate reduction of HH downstream targets (*GLI2*, *PTCH1* and *HHIP*) in NCI-H520 with a greater decrease in NCI-H226 and SK-MES-1 in comparison to DMSO control (Figure 23A~C). Western analysis confirmed the reduction of GLI2 protein in GANT61-treated cells (Figure 24). Consistent with previous apoptosis assay, cleaved caspase-3 was detected in cells receiving GANT61, evidence of the extensive apoptosis induced by GANT61 in GLI-positive cells (Figure 24). The expression of CCND1 was also decreased after GANT61 treatment in agreement with GLI2 reduction, indicating an impaired cell proliferation in addition to increased cell death (Figure 24).

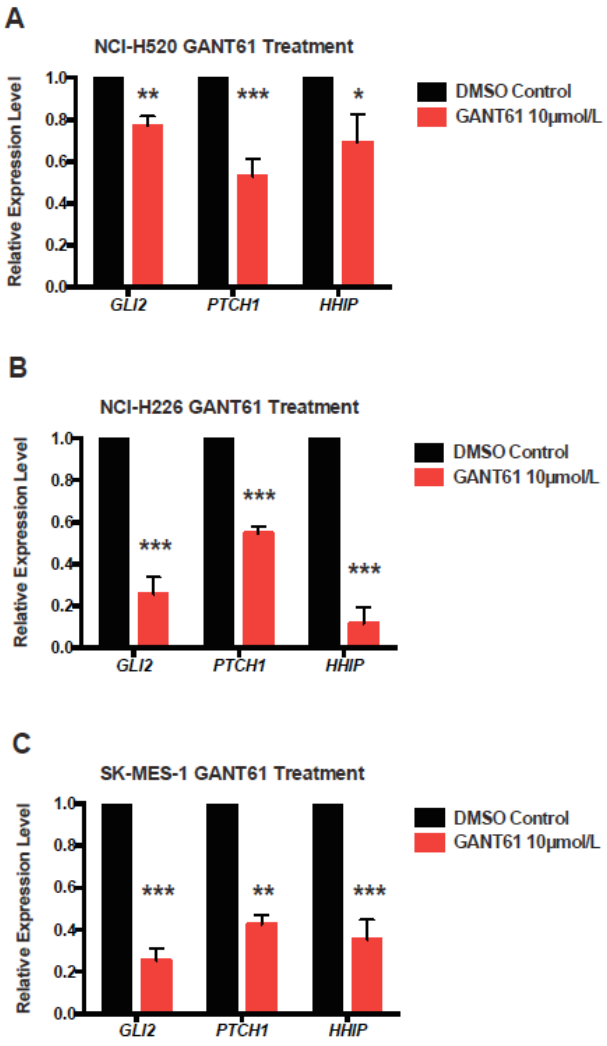


**Figure 23: Expression of HH target genes after GANT61 treatment**

Exposure to GANT61 reduced mRNA levels of GLI targets in GLI-positive cell lines: NCI-H520 (A), NCI-H226 (B), SK-MES-1 (C). Cells were treated with DMSO control or 10 μmol/L GANT61 for 96 hours. Gene expressions were normalized to endogenous *GAPDH* in each cell line. Data represent the mean ± SD of 3 independent experiments. Data were analyzed by two-tailed t test. (*: $p<0.05$; **: $p<0.01$; ***: $p<0.001$)

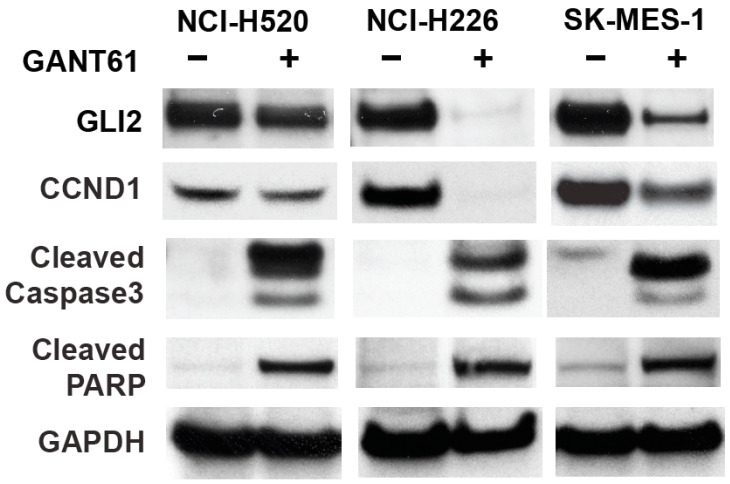


**Figure 24: GANT61 reduced expression of proliferation- and apoptosis- related genes**

96-hour treatment of GANT61 reduced expression of GLI2 and CCND1, and induced expression of cleaved caspase-3 and cleaved PARP, in comparison to DMSO control. GAPDH was used as the loading control. A representative Western blot from 3 independent experiments is shown.

## *5.3 Summary*

We have observed that suppression of SMO failed to reduce GLI2 expression, and showed no inhibition of downstream HH-GLI signaling. It suggested the existence of non-canonical regulation of GLI2 in LSCC cells via SMO-independent mechanisms. Therefore, we went on to test the importance of GLI2 in regulation of LSCC cell survival and cell death. GLI2 suppression by both shRNA knockdown and GANT61 treatment has resulted in strong growth inhibition and apoptosis induction in GLI2-expressing

LSCC cells. Expression of HH target genes downstream of GLI2, *PTCH1* and *HHIP*, has also been significantly reduced, indicating successful blockage of HH-GLI signaling. In addition, we have observed decreased CCND1 and induction of cleaved Caspase-3, cleaved PARP, which are consistent with reduced cell viability and increased cell death. While SMO plays a dispensable role in LSCC cells, GLI2 is required for cell survival and proliferation via mediating HH-GLI signaling, which raises the possibility that GLI2 may be a therapeutic target in LSCC. Importantly, GANT61 demonstrates great *in vitro* efficacy in growth inhibition and apoptosis induction in GLI-positive LSCC cells, and displays high degree of selectivity by showing no impacts in GLI-negative cells. In order to further test the potential of GLI2 inhibition in clinical care, we continue to investigate the efficacy of GANT61 *in vivo*.

# 6. GLI inhibitor GANT61 suppresses GLI-positive tumor progression *in vivo*.

## *6.1 Materials and Methods*

### 6.1.1 Xenograft and tumor treatment

$10^6$ NCI-H520 cells, $10^6$ NCI-H2170 cells or $5\times10^6$ NCI-H226 cells were suspended in a total volume of 100 μl of a 1:1 mixture of RPMI 1640 medium: Matrigel (BD Biosciences). Cells were injected subcutaneously in the right posterior flank of 6~8 week C.129S7 (B6)-*Rag1*$^{tm1Mom}$/ J (Rag1-/-) mice. Tumors were grown until they reached a median size of ≈250 $mm^3$ (NCI-H520), ≈230 $mm^3$ (NCI-H2170), and ≈150 $mm^3$ (NCI-H226). Animals were randomly divided into groups and treated with solvent only (corn oil: ethanol, 4:1) or GANT61 in solvent (50 mg/kg). Treatments were given every other day for 20 days by intraperitoneal injection. Tumor volumes were calculated by the formula $0.52\times\text{length}\times(\text{width})^2$. At the end of treatment, tumors were removed, weighed and processed for subsequent analysis. All animal experiments were approved by and conformed to the policies and regulations of Institutional Animal Care and Use Committees at Duke University. GANT61 was purchased from Sigma-Aldrich.

### 6.1.2 Tissue mRNA collection and quantitative real-time PCR

Fresh animal tissues were first excised and cut into slices less than 0.5 cm thick, and then immediately and completely submerged in the collection tubes containing RNA*later* RNA stabilization Reagent (Qiagen). Before RNA isolation, tissues were removed from RNA*later* RNA stabilization Reagent, and then disrupted and

homogenized. Total RNA was isolated using the Qiagen RNeasy Mini Kit, treated with DNase I (Invitrogen) and converted to cDNA using iScript cDNA Synthesis Kit (BIO-RAD). Real-time PCR was performed using TaqMan Gene Expression Master Mix on an Eppendorf Mastercycler, and raw data were analyzed by Realplex software. TaqMan probes for *PTCH1*, *HHIP* and *GAPDH* were purchased from Applied Biosystems.

## *6.2 Results*

### 6.2.1 GANT61 suppresses tumor growth of NCI-H520 *in vivo*.

Currently, there are no available transgenic murine models that faithfully recapitulate human LSCC. While *SOX2* is reported to be an amplified lineage-survival oncogene in human LSCC (6), overexpression of *Sox2* driven by several lung-cell-type specific Cre-promoters in mice produced adenocarcinoma (9). The *K-ras* $^{G12D}$ mutation combined with homozygous *Lkb1* inactivation generated a mixture of NSCLC, including LSCC, adenocarcinoma and large cell carcinoma (61). However, *K-Ras* mutation is rarely seen in LSCC patients (1). In recent years, patient-derived xenograft models of LSCC are of great interests, but have not achieved satisfactory progress. Therefore, we used a xenograft model of representative human LSCC cell lines to determine the efficacy of GANT61 in blocking HH-GLI signaling and subsequent tumor growth *in vivo*.

We first studied the *in vivo* efficacy of GANT61 on the xenografts of NCI-H520, which represents the classical subtype of LSCC and has high level of GLI2. NCI-H520 cancer cells were injected subcutaneously into the right flank of immune deficient Rag1-

/- mice. Mice were randomly divided into two groups when tumors reached median size of ≈250 $mm^3$ (n=8 for each group). We began treatment with either solvent control or GANT61 at a previously described dose of 50 mg/kg (51). In order to avoid severe ulcerations at the injection sites that occurred in a previous study, all injections were given intraperitoneally every other day. During a 20-day treatment period, suppression of NCI-H520 tumor growth was observed in the groups receiving GANT61 (Figure 25). Tumors of each group were removed and weighed at the end of the treatment. GANT61 led to a significant 40% reduction of tumor weight for NCI-H520 in comparison to the solvent control (Figure 26). No adverse side effects, such as weight loss, ulcerations, or general illness of the animals, were observed in either group during the entire treatment. Quantitative real-time PCR analysis of GLI targets in tumors confirmed that GANT61 significantly reduced the expression of the target genes *PTCH1* and *HHIP* (Figure 27), confirming an on-target anti-tumor activity of GANT61 *in vivo*. These data demonstrate that GANT61 is effective in inhibiting the growth of classical LSCC cell line via blocking HH-GLI signaling.

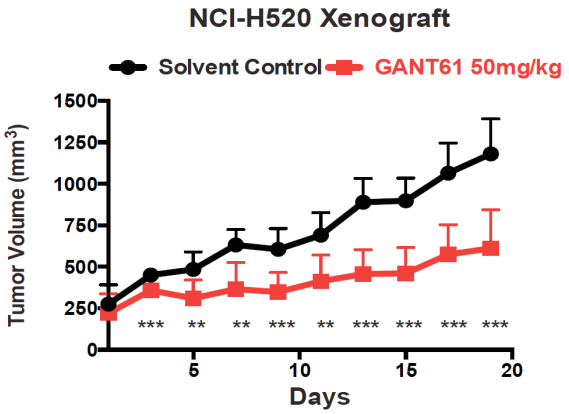


**Figure 25: Growth curve of NCI-H520 during GANT61 treatment**

Growth of NCI-H520 xenografts during treatment period is shown as the mean ± SD (n=8). Tumor volumes were calculated by the formula $0.52 \times \text{length} \times (\text{width})^2$. Data were analyzed by two-tailed t test. (**: $p<0.01$; ***: $p<0.001$.)

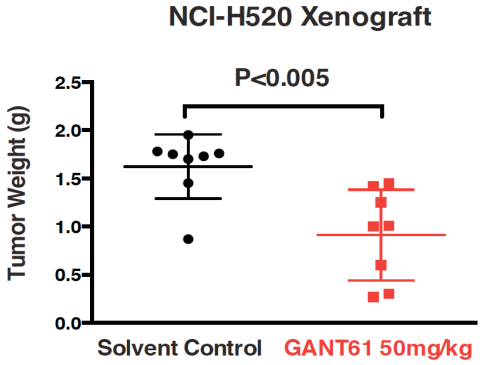


**Figure 26: Measurement of NCI-H520 tumor weight at the end of treatment**

Tumors from control and GANT61 treated groups (n=8) were removed and weighed at the end of treatment, and data were analyzed by two-tailed t test.

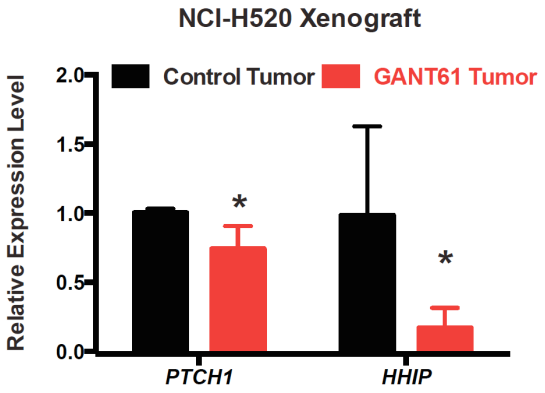


**Figure 27: Expression level of *PTCH1* and *HHIP* in NCI-H520 Xenografts**

Quantification of *PTCH1* and *HHIP* mRNA by real-time PCR in treated tumors for NCI-H520 (n=4). Values were normalized against *GAPDH*. Shown is the mean ± SD of independent tumors in each group. Data were analyzed by two-tailed t test (*: $p<0.05$).

### 6.2.2 GANT61 inhibits tumor growth of NCI-H226 *in vivo*.

Next, we evaluated the *in vivo* efficacy of GANT61 on the xenografts of NCI-H226. Although NCI-H226 is predicted to be the secretory subtype of LSCC, it exhibits endogenous high level of GLI2 expression. NCI-H226 cancer cells were injected subcutaneously into the right flank of immune deficient Rag1-/- mice. Mice were randomly divided into two groups when tumors reached median size of ≈150 $mm^3$ (n=5 for each group). Treatment was started with either solvent control or GANT61 (50 mg/kg) by intraperitoneal injection every other day. During a 20-day treatment period, inhibition of tumor growth was observed in NCI-H226 xenograft tumors receiving GANT61 (Figure 28). In the end of treatment, GANT61 resulted in a significant 40%

reduction of NCI-H226 tumor weight when compared with tumors receiving solvent control (Figure 29). No adverse side effects, such as weight loss, ulcerations, or general illness of the animals, were observed in either group during the entire treatment. Expression of *PTCH1* and *HHIP* in GANT61-treated tumors was significantly decreased in comparison to the control group (Figure 30). Taken together, these studies show that GANT61 is effective in suppressing the progression of secretory LSCC tumors with high GLI2 via blockage of HH-GLI signaling.

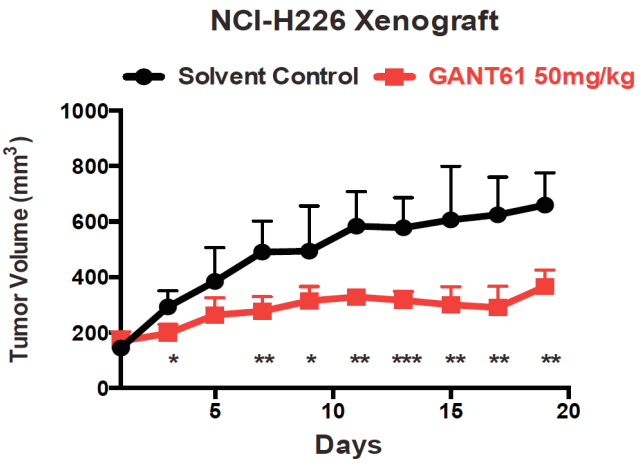


**Figure 28: Growth curve of NCI-H226 during GANT61 treatment**

Growth of NCI-H226 xenografts during treatment period is shown as the mean ± SD (n=5). Tumor volumes were calculated by the formula 0.52×length×(width)$^2$. Data were analyzed by two-tailed t test. (*: $p$<0.05; **: $p$<0.01; ***: $p$<0.001)

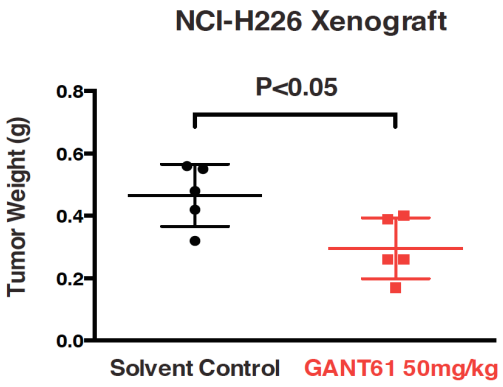


**Figure 29: Measurement of NCI-H226 tumor weight at the end of treatment**

Tumors from control and GANT61 treated groups (n=5) were removed and weighed at the end of treatment, and data were analyzed by two-tailed t test.

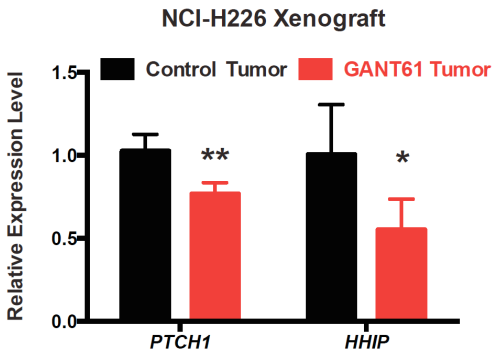


**Figure 30: Expression level of *PTCH1* and *HHIP* in NCI-H226 xenografts**

Quantification of *PTCH1* and *HHIP* mRNA by real-time PCR in treated tumors for NCI-H226 (n=5). Values were normalized against *GAPDH*. Shown is the mean ± SD of independent tumors in each group. Data were analyzed by two-tailed t test (*: $p<0.05$, **: $p<0.01$).

### 6.2.3 Growth of GLI-negative NCI-H2170 was not affected by GANT61 *in vivo*.

Off-target toxicity is a big concern in therapeutic agent development. In order to test the selectivity and efficacy of GANT61 *in vivo*, a xenograft model of GLI-negative NCI-H2170 was established by injecting cancer cells subcutaneously into the right flank of immune deficient Rag1-/- mice. Mice were randomly divided into two groups when tumors reached median size of ≈230 $mm^3$ (n=5 for each group). We began treatment with either solvent control or GANT61 (50 mg/kg) by intraperitoneal injection every other day as performed in NCI-H520 and NCI-H226 xenografts. During a 20-day treatment, however, no significant difference of tumor growth was found in the NCI-H2170 xenograft (Figure 31). In contrast to GLI-positive NCI-H520 and NCI-H226, no significant reduction of tumor volume or tumor weight was observed in the GLI-negative NCI-H2170 tumors (Figure 32), suggesting a specific anti-tumor efficacy of GANT61 in GLI overexpressing cancer cells. Consistently, expression level of GLI targets, *PTCH1* and *HHIP*, was not significantly changed in GANT61-treated NCI-H2170 xenograft tumors (Figure 33).

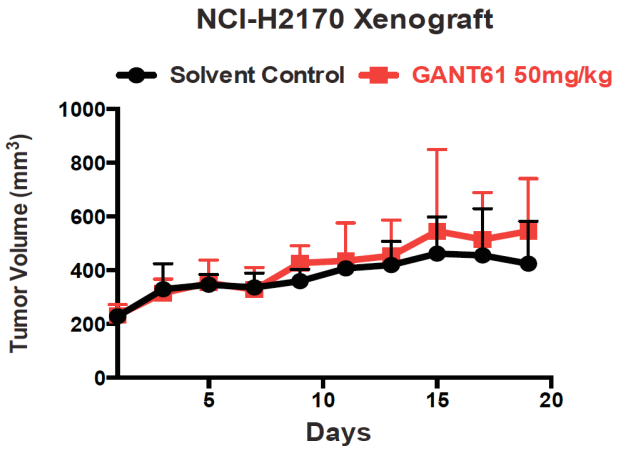


**Figure 31: Growth curve of NCI-H2170 during GANT61 treatment**

Growth of NCI-H2170 xenografts during treatment period is shown as the mean ± SD (n=5). Tumor volumes were calculated by the formula $0.52 \times \text{length} \times (\text{width})^2$. Data were analyzed by two-tailed t test. No significant difference of tumor growth was observed between control group and GANT61 group.

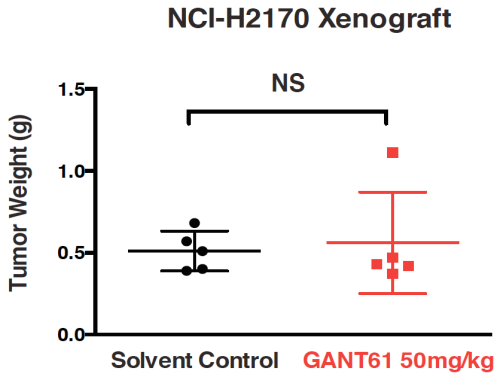


**Figure 32: Measurement of NCI-H2170 tumor weight at the end of treatment**

Tumors from control and GANT61 treated groups (n=5) were weighed at the end of treatment. Data were analyzed by two-tailed t test, NS: not significant.

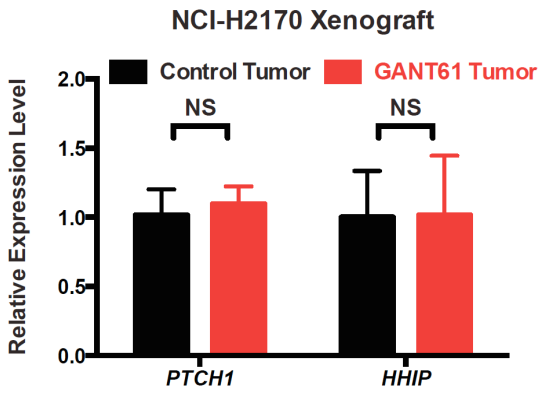


**Figure 33: Expression Level of *PTCH1* and *HHIP* in NCI-H2170 xenografts**

Quantification of *PTCH1* and *HHIP* mRNA by real-time PCR in treated tumors for NCI-H2170 (n=5). Values were normalized against *GAPDH*. Shown is the mean ± SD of independent tumors in each group. Data were analyzed by two-tailed t test: NS: not significant.

## *6.3 Summary*

Based on our *in vitro* studies, we expected that the *in vivo* tumor growth of SK-MES-1 would also be suppressed by GANT61 treatment. In our studies, $5\times10^6$ SK-MES-1 cells with Matrigel were subcutaneously injected into the right flank of Rag1-/- mice (n=10). However, after more than 10 weeks, no palpable tumor was established in these mice. This experiment was repeated in another four mice, but again no tumors were successfully established for this cell line. This is not surprising because we also noticed that *in vitro* growth of SK-MES-1 is much slower than the other three cell lines. Since this cell line appeared to be difficult to form xenograft tumors, we chose to test two GLI-

positive cell lines, NCI-H520 and NCI-H226, as well as one GLI-negative cell line NCI-H2170.

Consistent with the *in vitro* studies, GANT61 suppresses *in vivo* tumor progression of GLI-positive LSCC cell lines, NCI-H520 and NCI-H226, during treatment period, and leads to significant reduction of final tumor weights. As expected, growth of GLI-negative NCI-H2170 xenografts is not affected by GANT61, again demonstrating the high selectivity of GANT61. Expression of HH-GLI target genes, PTCH1 and HHIP, in NCI-H520 and NCI-H226 is significantly decreased, but is no influenced in NCI-H2170, suggesting that GANT61 maintains robust efficacy and selectivity of inhibiting HH-GLI signaling *in vivo*. These data suggest the potential clinical application of GLI inhibition by GANT61 in treating patients with HH-GLI active LSCC.

# 7. Conclusion, discussion and future directions

## *7.1 Conclusions*

Aberrant HH signaling has been implicated in a diverse spectrum of human cancers. Previous studies have reported hyperactive HH signaling in a subset of LSCC, but they failed to address the complexity and heterogeneity of the disease. Four distinct molecular subtypes, which have different survival outcomes, patient populations, and biological processes, were identified by gene expression-subtype signatures (19).

In the recent study of TCGA (20), we found that the HH activation is associated with the classical subtype (~36% of LSCC), and approximate 55% of the classical subtype displayed high expression of *GLI2*. A consistent pattern was observed in an independent UNC microarray dataset. This observation is consistent with previous immunohistochemical studies, which showed high activation of HH signaling in approximately 27% of LSCC patients (41, 42). Among all four subtypes, the classical subtype has the highest proportion of smokers and the heaviest smoking history, as well as the greatest overexpression of three known oncogenes on 3q26 amplicon: *SOX2*, *TP63* and *PIK3CA* (19, 20). While *GLI2* was consistently highly expressed in the classical subtype, strong positive correlations between *GLI2* and the three best-known markers of the classical subtype on chromosome 3q were observed, together suggesting a critical role of *GLI2* in LSCC, as found in SCC in other organs (44-46). If the hyperactive HH-GLI signaling found in the classical subtype of LSCC is required for tumor maintenance and

progression, suppressing the HH-GLI pathway by clinically-available inhibitors may be a potent targeted therapy to treat a subset of LSCC patients.

Recent development of multiple SMO inhibitors for human administration prompted us to test the potential clinical application to treat LSCC patients by targeting SMO. However, shRNAs knockdown of SMO showed only minor effects on LSCC cell survival and apoptosis, with little effect on HH downstream target gene expression. Consistently, GDC-0449 produced limited cytotoxicity despite the universal expression of SMO, suggesting the existence of SMO-independent regulation of GLI signaling. The strong and unique expression pattern of *GLI2* prompted the query whether it is necessary for LSCC tumor progression. Knockdown of GLI2 induced apoptosis and significant growth inhibition in GLI2-positive LSCC cells, demonstrating an essential role of GLI2 in regulating cell viability and death. Importantly, the GLI inhibitor, GANT61, effectively blocked GLI-mediated signal transduction and suppressed tumor growth both *in vitro* and *in vivo*. Recent studies in neuroblastoma (55) and chronic lymphocytic leukemia (56) also showed that GANT61 effectively suppressed tumor progression in cancers insensitive to SMO inhibition. Interestingly, amplification of *GLI2* or *CCND1* have been proposed as additional mechanisms responsible for resistance to SMO inhibitors (50), and GANT61 treatment significantly reduced expression of GLI2 and CCND1 in LSCC cells.

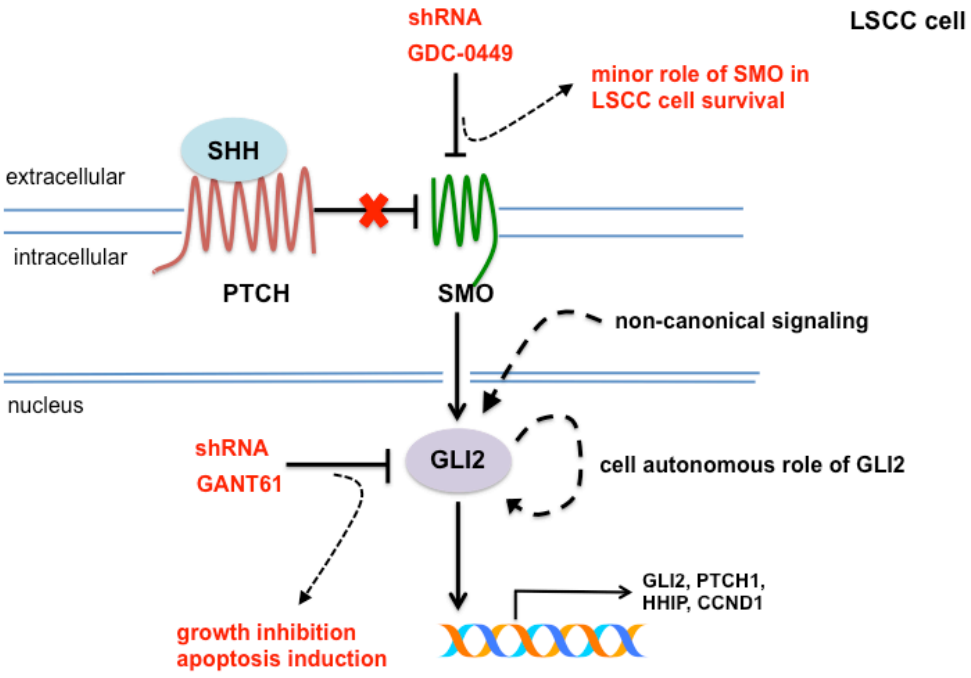


**Figure 34: A hypothetical model of the HH-GLI pathway in LSCC**

Canonical HH-GLI signaling is activated by the ligand-dependent activation of SMO. However, direct and specific inhibition of SMO in LSCC cells has little impacts on downstream signaling and cell survival. In contrast, direct knockdown or specific blockage of GLI2 results in growth inhibition and apoptosis induction, suggesting a critical role of GLI2 in LSCC. GLI2 may be activated in a cell autonomous fashion and/or through non-canonical HH signaling.

As summarized in Figure 34, we have identified SMO-independent GLI regulation in LSCC, and demonstrated that GLI2 is important for cell survival and

proliferation. Treatment options for LSCC overall are disappointing. Different from standard-of-care chemotherapy or small molecule inhibition of kinase signaling cascades, we present a novel and potential strategy to treat a subset of LSCC patients by targeting the GLI transcriptional network. Our studies also highlight the need for agents that suppress GLI effectors with high efficacy and selectivity.

## *7.2 Discussion and Future Directions*

### 7.2.1 Non-canonical activation of GLI signaling in LSCC

The canonical activation of HH-GLI signaling is initiated by the binding of HH ligands to the receptor PTCH, and thus relieves the repression of PTCH on SMO, which further triggers a series of cellular events and leads to GLI activation. Interestingly, we notice that the expression of ligand *SHH* within the classical subtype varied markedly and was not significantly different between subtypes. The expression patterns of other two HH ligands, *IHH* and *DHH*, were similar to *SHH* (Figure 35). These data indicate the existence of ligand-independent GLI activation in the classical subtype. Genetic alterations, including loss of PTCH function, constitutively active SMO, and amplification of *GLI1*/*GLI2* have been reported to activate downstream HH signaling independent of ligands in various cancers. Moreover, GLI function can be modulated in a SMO-independent manner by PI3K/AKT (30), RAS-MEK signaling (31, 32), which may contribute to the hyperactive HH-GLI signaling in LSCC in addition to canonical HH signaling.

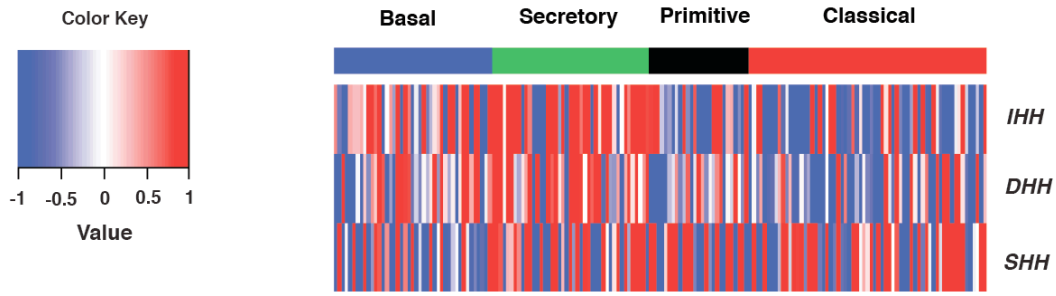


**Figure 35: Expression pattern of HH ligands in four LSCC subtypes of the TCGA cohort**

Tumor samples are displayed as columns, grouped by gene expression subtype. Selected HH ligands are shown in rows.

While RAS mutation is rarely seen in LSCC, *PIK3CA* copy number gains and loss of *PTEN* function are prevalent in the classical subtype of LSCC, where the activation of HH signaling was observed. GLI2 exhibits a strong positive correlation with *PIK3CA* expression. It has been shown that PI3K/AKT pathway positively regulates HH-GLI signaling by inhibiting Protein Kinase A (PKA)-mediated degradation of GLI2 (30). NCI-H520, representing the classical subtype of LSCC, has been reported to harbor *PIK3CA* amplification and *PTEN* loss-of-function mutation, and thus has endogenous active PI3K signaling (62). Growth of NCI-H520 can be significantly inhibited by a pan PI3K inhibitor GDC-0941 or a dual PI3K/mTOR inhibitor GDC-0980 both *in vitro* and *in vivo* (62). Our preliminary data suggested that the treatment of a classical PI3K inhibitor in NCI-H520 cells significantly reduced *GLI2* mRNA level. Therefore, an attractive

hypothesis that explains the ligand/receptor-independent activation of GLI in the classical subtype of LSCC could be that the constitutively active PI3K/AKT signaling caused by *PIK3CA* amplification or *PTEN* mutation leads to GLI2 activation in addition to the canonical PI3K-AKT-mTOR signaling cascade. Although GANT61 can significantly decrease GLI2 expression in NCI-H520 cells, we notice that this reduction is greater in NCI-H226 cell line, which is classified as a *PIK3CA*-wild-type line with low baseline level of PI3K/AKT signaling (12). It is likely that when GANT61 lowers the binding capacity of GLI2 to DNA and therefore reduces the feedback production of GLI2, endogenously active PI3K signaling is able to compensate the partial loss of GLI2 by suppressing GLI2 degradation and even upregulating GLI2 expression. Therefore, we are currently studying the role of PI3K/AKT signaling in regulation of GLI2 in the classical subtype of LSCC.

### 7.2.2 Other potential GLI inhibitors

An important question in the clinical setting is to determine which patient should receive GLI inhibitor treatment. In the TCGA cohort, we observed strong positive correlation between *PTCH1* and *GLI2* (Figure 36), indicating that samples with high *GLI2* tend to have high *PTCH1*, and vice versa. Therefore, upregulation of either *PTCH1* or *GLI2* can be used to determine the HH signaling activation. Since GLI1 may conduct overlapping functions of GLI2, and GANT61 can inhibit both GLI1- and GLI2-mediated transcription, we believe that the expression of GLI1 should also be tested in

patient specimens. In the clinical setting, immunohistochemistry staining for *PTCH1*, *GLI2* and *GLI1* can be performed in patient specimens to identify HH-GLI active patient tumors as demonstrated by previous studies shown in Figure 3 (41, 42), which show that HH signaling components are overexpressed in LSCC, but absent from the adjacent non-neoplastic lung parenchyma. Patients with hyperactive HH-GLI signaling should be more likely to respond to GLI inhibition therapy.

Our findings highlight the need for agents that suppress downstream GLI effectors with high efficacy and selectivity. GANT61 is a relatively new member in the HH inhibitor family, since most known HH pathway antagonists focus on the transmembrane activator SMO. Other readily available agents that inhibit GLI2 are rare. Arsenic trioxide (ATO), which is FDA-approved treatment for acute promyelocytic leukemia, has recently been described as a potent HH inhibitor. ATO has been shown to inhibit HH signaling by inhibiting GLI2 ciliary accumulation and promoting its degradation (63). It has recently been shown to actively inhibit tumor growth in known drug-resistant SMO mutations of medulloblastoma and basal cell carcinoma and in the context of GLI2 overexpression (64). Due to the likelihood that compounds that block HH pathway-dependent proliferation in one cell type may be inactive in others, the clinical relevance of ATO in LSCC treatment is currently under investigation.

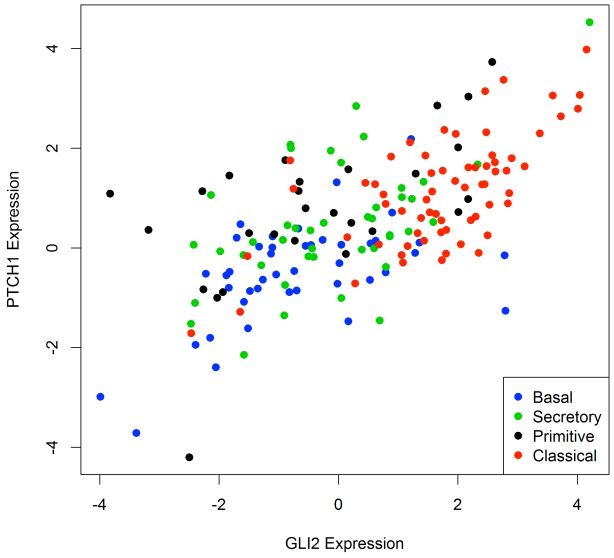


**Figure 36: Scatterplot of *GLI2* and *PTCH1* expression in the TCGA cohort**

Gene expression values for *GLI2* and *PTCH1* from the TCGA cohort are plotted and colored according to their gene expression subtype. The expression values for these two genes exhibit a strong positive association, as evidenced by the high positive value of the Spearman correlation coefficient ($r^2 = 0.61$).

### 7.2.3 Combined therapy of GLI inhibition, PI3K/AKT suppression, and cisplatin

A recently emerging idea in clinical treatment is to combine several anti-tumor agents that specifically target different signaling pathways. It has been reported that GLI function can be modulated in a SMO-independent manner by PI3K/AKT signaling (30). Pharmacologic inhibition of PI3K/AKT signaling reduced tumor growth in GDC-0449-resistant medulloblastoma (50). Several inhibitors of the PI3K pathway are undergoing

clinical evaluation. *PIK3CA* copy number gains and loss of *PTEN* function are prevalent in the classical subtype of LSCC, where the activation of HH signaling was observed. We speculate that the endogenously active PI3K/AKT signaling in the classical subtype of LSCC can positively regulate GLI expression and activity. This coexistence raises the possibility that a combined therapy of GLI inhibition and PI3K/AKT suppression may be more beneficial than a monotherapy to enhance efficiency and overcome drug resistance in patients. It is also likely that treatment of GLI inhibitors and PI3K/AKT inhibitors may increase the susceptibility cancer cells to conventional chemotherapy. Cisplatin, which causes cross-linking of DNA and ultimately triggers apoptosis, is a conventional platinum-containing chemotherapy drug for treating LSCC. Despite its ability to induce DNA damage, cisplatin has a number of side effects due to the general cytotoxicity. The majority of cancer patients will eventually relapse with cisplatin-resistant disease even if initial platinum responsiveness is high. Many mechanisms of cisplatin resistance have been proposed including changes in cellular uptake and efflux of the drug, increased detoxification of the drug, inhibition of apoptosis and increased DNA repair (65). Solid tumors, including LSCC, are highly heterogeneous. The actively proliferating cancer cells are usually considered to have aberrant oncogenic stimuli. However, the stroma, which creates supporting microenvironment, is likely to be formed by normal cells, such as blood cells, immune cells and fibroblasts, and thus may be less sensitive to specific

pathway inhibitors. Therefore, eliminating these stromal cells with cisplatin may help to enhance the targeting efficacy of GLI or other pathway inhibitors.

Taken together, there are two aspects we would like to study for potential clinical application: (1) Combination of GLI inhibitor and PI3K/AKT inhibitor in LSCC cells with GLI overexpression and hyperactive PI3K/AKT signaling. (2) Cisplatin treatment plus either GLI inhibitor, or PI3K/AKT inhibitor, or both.

### 7.2.4 Patient-derived xenograft models of LSCC

Established cancer cell lines provide convenience for *in vitro* studies, particularly for those cancers that are very difficult to adapt to *in vitro* culture system. We have observed significant efficacy of GLI inhibitor GANT61 in representative LSCC cell lines both *in vitro* and *in vivo*. However, these cells may have accumulated various mutations rarely seen *in vivo* due to multiple passages, and further become independent of or less sensitive to a signaling pathway essential for *in vivo* survival. Moreover, the limited number of available cell lines may not faithfully represent the diversity of patient populations and biological backgrounds. These shortcomings of using cancer cell lines highlight the need to establish an *in vivo* system that can directly and successfully propagate the primary tumors dissected from patients.

LSCC has long been known as being difficult to adapt to immunodeficient mice with a substantially low tumor take rate. In collaboration with other laboratories and Duke Core Facility, we are trying to collect a large amount of LSCC samples and

develop a system in which the fresh LSCC tumor is minced and transplanted subcutaneously into Rag1-/- mice. A few number of primary LSCC may be successfully passaged. Over a period of weeks, tumors start to grow and later are propagated to more new Rag1-/- mice. Tumors multiplied in mice have been shown to better maintain histological features and the gene expression pattern at both message and protein levels (66). Furthermore, patient-derived xenograft tumors maintain at least some aspects of the human microenvironment for weeks with the complete substitution with murine stroma occurring only after 2-3 passages in mouse (66), which therefore represents a more realistic model for preclinical evaluation on drug development. This system will enable us to conduct *in vivo* drug tests across a broad spectrum of original patient samples.

After tumor samples are harvested in the operating room, a small portion of tumor tissues will be immediately processed for mRNA and protein extraction, while the remaining will be used for *in vivo* passage. The expression level of GLI1 and GLI2 can be evaluated by Real-time PCR or Western blot. Section slides can be obtained from pathology department after histology of the tumor is determined. We, therefore, will be able to identify tumors with hyperactive HH-GLI signaling and potentially other active oncogenic pathways. Based on our genomic analysis and previous IHC studies, we anticipate approximately 20%~30% of primary LSCC expressing high level of GLIs. The

xenograft tumors of these GLI-positive samples can be used to assess the therapeutic efficacy of GLI inhibitor(s) and/or combined therapies.

# References

1. Drilon A, Rekhtman N, Ladanyi M, Paik P. Squamous-cell carcinomas of the lung: emerging biology, controversies, and the promise of targeted therapy. The Lancet Oncology. 2012;13(10):e418-e26.

2. Pennell NA. Selection of chemotherapy for patients with advanced non–small cell lung cancer. Cleveland Clinic Journal of Medicine. 2012;79(e-Suppl 1):e-S46-e-S50.

3. Gontan C, de Munck A, Vermeij M, Grosveld F, Tibboel D, Rottier R. Sox2 is important for two crucial processes in lung development: Branching morphogenesis and epithelial cell differentiation. Developmental Biology. 2008;317(1):296-309.

4. Tompkins DH, Besnard Vr, Lange AW, Wert SE, Keiser AR, Smith AN, et al. Sox2 Is Required for Maintenance and Differentiation of Bronchiolar Clara, Ciliated, and Goblet Cells. PLos One. 2009;4(12):e8248.

5. Que J, Luo X, Schwartz RJ, Hogan BLM. Multiple roles for Sox2 in the developing and adult mouse trachea. Development. 2009;136(11):1899-907.

6. Bass AJ, Watanabe H, Mermel CH, Yu S, Perner S, Verhaak RG, et al. SOX2 is an amplified lineage-survival oncogene in lung and esophageal squamous cell carcinomas. Nat Genet. 2009;41(11):1238-42.

7. Hussenet T, Dali S, Exinger J, Monga B, Jost B, Dembelé D, et al. SOX2 Is an Oncogene Activated by Recurrent 3q26.3 Amplifications in Human Lung Squamous Cell Carcinomas. PLos One. 2010;5(1):e8960.

8. Maier S, Wilbertz T, Braun M, Scheble V, Reischl M, Mikut R, et al. SOX2 amplification is a common event in squamous cell carcinomas of different organ sites. Human Pathology. 2011;42(8):1078-88.

9. Lu Y, Futtner C, Rock JR, Xu X, Whitworth W, Hogan BLM, et al. Evidence That SOX2 Overexpression Is Oncogenic in the Lung. PLos One. 2010;5(6):e11022.

10. Shibata T, Ohta T, Tong KI, Kokubu A, Odogawa R, Tsuta K, et al. Cancer related mutations in NRF2 impair its recognition by Keap1-Cul3 E3 ligase and promote malignancy. Proceedings of the National Academy of Sciences. 2008;105(36):13568-73.

11. Kim YR, Oh JE, Kim MS, Kang MR, Park SW, Han JY, et al. Oncogenic NRF2 mutations in squamous cell carcinomas of oesophagus and skin. The Journal of Pathology. 2010;220(4):446-51.

12. Yamamoto H, Shigematsu H, Nomura M, Lockwood WW, Sato M, Okumura N, et al. PIK3CA Mutations and Copy Number Gains in Human Lung Cancers. Cancer Research. 2008;68(17):6913-21.

13. Okudela K, Suzuki M, Kageyama S, Bunai T, Nagura K, Igarashi H, et al. PIK3CA mutation and amplification in human lung cancer. Pathology International. 2007;57(10):664-71.

14. Ji M, Guan H, Gao C, Shi B, Hou P. Highly frequent promoter methylation and PIK3CA amplification in non-small cell lung cancer (NSCLC). BMC Cancer. 2011;11(1):147.

15. Jin G, Kim MJ, Jeon H-S, Choi JE, Kim DS, Lee EB, et al. PTEN mutations and relationship to EGFR, ERBB2, KRAS, and TP53 mutations in non-small cell lung cancers. Lung cancer (Amsterdam, Netherlands). 2010;69(3):279-83.

16. Weiss J, Sos ML, Seidel D, Peifer M, Zander T, Heuckmann JM, et al. Frequent and Focal FGFR1 Amplification Associates with Therapeutically Tractable FGFR1 Dependency in Squamous Cell Lung Cancer. Science Translational Medicine. 2010;2(62):62ra93.

17. Dutt A, Ramos AH, Hammerman PS, Mermel C, Cho J, Sharifnia T, et al. Inhibitor-Sensitive *FGFR1* Amplification in Human Non-Small Cell Lung Cancer. PLos One. 2011;6(6):e20351.

18. Hammerman PS, Sos ML, Ramos AH, Xu C, Dutt A, Zhou W, et al. Mutations in the DDR2 Kinase Gene Identify a Novel Therapeutic Target in Squamous Cell Lung Cancer. Cancer Discovery. 2011;1(1):78-89.

19. Wilkerson MD, Yin X, Hoadley KA, Liu Y, Hayward MC, Cabanski CR, et al. Lung Squamous Cell Carcinoma mRNA Expression Subtypes Are Reproducible, Clinically Important, and Correspond to Normal Cell Types. Clinical Cancer Research. 2010;16(19):4864-75.

20. Comprehensive genomic characterization of squamous cell lung cancers. Nature. 2012;489(7417):519-25.

21. di Magliano MP, Hebrok M. Hedgehog signalling in cancer formation and maintenance. Nat Rev Cancer. 2003;3(12):903-11.

22. Ruiz i Altaba A, Mas C, Stecca B. The Gli code: an information nexus regulating cell fate, stemness and cancer. Trends in Cell Biology. 2007;17(9):438-47.

23. Thiyagarajan S, Bhatia N, Reagan-Shaw S, Cozma D, Thomas-Tikhonenko A, Ahmad N, et al. Role of GLI2 Transcription Factor in Growth and Tumorigenicity of Prostate Cells. Cancer Research. 2007;67(22):10642-6.

24. Ikram MS, Neill GW, Regl G, Eichberger T, Frischauf A-M, Aberger F, et al. GLI2 Is Expressed in Normal Human Epidermis and BCC and Induces GLI1 Expression by Binding to its Promoter. J Investig Dermatol. 2004;122(6):1503-9.

25. Bai CB, Auerbach W, Lee JS, Stephen D, Joyner AL. Gli2, but not Gli1, is required for initial Shh signaling and ectopic activation of the Shh pathway. Development. 2002;129(20):4753-61.

26. Eichberger T, Sander V, Schnidar H, Regl G, Kasper M, Schmid C, et al. Overlapping and distinct transcriptional regulator properties of the GLI1 and GLI2 oncogenes. Genomics. 2006;87(5):616-32.

27. Duman-Scheel M, Weng L, Xin S, Du W. Hedgehog regulates cell growth and proliferation by inducing Cyclin D and Cyclin E. Nature. 2002;417(6886):299-304.

28. Bigelow RLH, Chari NS, Undén AB, Spurgers KB, Lee S, Roop DR, et al. Transcriptional Regulation of bcl-2 Mediated by the Sonic Hedgehog Signaling Pathway through gli-1. Journal of Biological Chemistry. 2004;279(2):1197-205.

29. Regl G, Kasper M, Schnidar H, Eichberger T, Neill GW, Philpott MP, et al. Activation of the BCL2 Promoter in Response to Hedgehog/GLI Signal Transduction Is Predominantly Mediated by GLI2. Cancer Research. 2004;64(21):7724-31.

30. Riobó NA, Lu K, Ai X, Haines GM, Emerson CP. Phosphoinositide 3-kinase and Akt are essential for Sonic Hedgehog signaling. Proceedings of the National Academy of Sciences of the United States of America. 2006;103(12):4505-10.

31. Stecca B, Mas C, Clement V, Zbinden M, Correa R, Piguet V, et al. Melanomas require HEDGEHOG-GLI signaling regulated by interactions between GLI1 and the RAS-MEK/AKT pathways. Proceedings of the National Academy of Sciences. 2007;104(14):5895-900.

32. Nolan-Stevaux O, Lau J, Truitt ML, Chu GC, Hebrok M, Fernández-Zapico ME, et al. GLI1 is regulated through Smoothened-independent mechanisms in neoplastic pancreatic ducts and mediates PDAC cell survival and transformation. Genes & Development. 2009;23(1):24-36.

33. Pepicelli CV, Lewis PM, McMahon AP. Sonic hedgehog regulates branching morphogenesis in the mammalian lung. Current Biology. 1998;8(19):1083-6.

34. Bellusci S, Furuta Y, Rush MG, Henderson R, Winnier G, Hogan BL. Involvement of Sonic hedgehog (Shh) in mouse embryonic lung growth and morphogenesis. Development. 1997;124(1):53-63.

35. Litingtung Y, Lei L, Westphal H, Chiang C. Sonic hedgehog is essential to foregut development. Nat Genet. 1998;20(1):58-61.

36. Park HL, Bai C, Platt KA, Matise MP, Beeghly A, Hui CC, et al. Mouse Gli1 mutants are viable but have defects in SHH signaling in combination with a Gli2 mutation. Development. 2000;127(8):1593-605.

37. Motoyama J, Liu J, Mo R, Ding Q, Post M, Hui C-c. Essential function of Gli2 and Gli3 in the formation of lung, trachea and oesophagus. Nat Genet. 1998;20(1):54-7.

38. Katoh Y, Katoh M. Hedgehog Target Genes: Mechanisms of Carcinogenesis Induced by Aberrant Hedgehog Signaling Activation. Current Molecular Medicine. 2009;9(7):873-86.

39. Watkins DN, Berman DM, Burkholder SG, Wang B, Beachy PA, Baylin SB. Hedgehog signalling within airway epithelial progenitors and in small-cell lung cancer. Nature. 2003;422(6929):313-7.

40. Park K-S, Martelotto LG, Peifer M, Sos ML, Karnezis AN, Mahjoub MR, et al. A crucial requirement for Hedgehog signaling in small cell lung cancer. Nat Med. 2011;17(11):1504-8.

41. Gialmanidis IP, Bravou V, Amanetopoulou SG, Varakis J, Kourea H, Papadaki H. Overexpression of hedgehog pathway molecules and FOXM1 in non-small cell lung carcinomas. Lung Cancer. 2009;66(1):64-74.

42. Raz G, Allen KE, Kingsley C, Cherni I, Arora S, Watanabe A, et al. Hedgehog signaling pathway molecules and ALDH1A1 expression in early-stage non-small cell lung cancer. Lung Cancer. 2012;76(2):191-6.

43. Shi I, Sadraei NH, Duan Z-H, Shi T, Shi I, Sadraei NH, et al. Aberrant Signaling Pathways in Squamous Cell Lung Carcinoma. Cancer Informatics. 2011;10(2923-CIN-Aberrant-Signaling-Pathways-in-Squamous-Cell-Lung-Carcinoma2.pdf):273-85.

44. Snijders AM, Schmidt BL, Fridlyand J, Dekker N, Pinkel D, Jordan RCK, et al. Rare amplicons implicate frequent deregulation of cell fate specification pathways in oral squamous cell carcinoma. Oncogene. 2005;24(26):4232-42.

45. Yan M, Wang L, Zuo H, Zhang Z, Chen W, Mao L, et al. HH/GLI signalling as a new therapeutic target for patients with oral squamous cell carcinoma. Oral Oncology. 2011;47(6):504-9.

46. Yang L, Wang L-S, Chen XL, Gatalica Z, Qiu S, Liu Z, et al. Hedgehog signaling activation in the development of squamous cell carcinoma and adenocarcinoma of esophagus. Int J Biochem Mol Biol. 2012;3(1):46-57. Epub 2012 Feb 10th.

47. Rudin CM, Hann CL, Laterra J, Yauch RL, Callahan CA, Fu L, et al. Treatment of Medulloblastoma with Hedgehog Pathway Inhibitor GDC-0449. New England Journal of Medicine. 2009;361(12):1173-8.

48. Von Hoff DD, LoRusso PM, Rudin CM, Reddy JC, Yauch RL, Tibes R, et al. Inhibition of the Hedgehog Pathway in Advanced Basal-Cell Carcinoma. New England Journal of Medicine. 2009;361(12):1164-72.

49. Yauch RL, Dijkgraaf GJP, Alicke B, Januario T, Ahn CP, Holcomb T, et al. Smoothened Mutation Confers Resistance to a Hedgehog Pathway Inhibitor in Medulloblastoma. Science. 2009;326(5952):572-4.

50. Dijkgraaf GJP, Alicke B, Weinmann L, Januario T, West K, Modrusan Z, et al. Small Molecule Inhibition of GDC-0449 Refractory Smoothened Mutants and Downstream Mechanisms of Drug Resistance. Cancer Research. 2011;71(2):435-44.

51. Lauth M, Bergström Å, Shimokawa T, Toftgård R. Inhibition of GLI-mediated transcription and tumor cell growth by small-molecule antagonists. Proceedings of the National Academy of Sciences. 2007;104(20):8455-60.

52. Mazumdar T, DeVecchio J, Shi T, Jones J, Agyeman A, Houghton JA. Hedgehog Signaling Drives Cellular Survival in Human Colon Carcinoma Cells. Cancer Research. 2011;71(3):1092-102.

53. Mazumdar T, DeVecchio J, Agyeman A, Shi T, Houghton JA. Blocking Hedgehog Survival Signaling at the Level of the GLI Genes Induces DNA Damage and Extensive Cell Death in Human Colon Carcinoma Cells. Cancer Research. 2011;71(17):5904-14.

54. Fu J, Rodova M, Roy SK, Sharma J, Singh KP, Srivastava RK, et al. GANT-61 inhibits pancreatic cancer stem cell growth in vitro and in NOD/SCID/IL2R gamma null mice xenograft. Cancer letters. 2013;330(1):22-32.

55. Wickström M, Dyberg C, Shimokawa T, Milosevic J, Baryawno N, Fuskevåg OM, et al. Targeting the hedgehog signal transduction pathway at the level of GLI inhibits neuroblastoma cell growth in vitro and in vivo. International Journal of Cancer. 2013;132(7):1516-24.

56. Desch P, Asslaber D, Kern D, Schnidar H, Mangelberger D, Alinger B, et al. Inhibition of GLI, but not Smoothened, induces apoptosis in chronic lymphocytic leukemia cells. Oncogene. 2010;29(35):4885-95.

57. Li B, Dewey C. RSEM: accurate transcript quantification from RNA-Seq data with or without a reference genome. BMC Bioinformatics. 2011;12(1):323.

58. R Core Team (2012). R: A language and environment for statistical computing. R Foundation for Statistical Computing V, Austria. ISBN 3-900051-07-0, URL http://www.R-project.org.

59. Barretina J, Caponigro G, Stransky N, Venkatesan K, Margolin AA, Kim S, et al. The Cancer Cell Line Encyclopedia enables predictive modelling of anticancer drug sensitivity. Nature. 2012;483(7391):603-307.

60. Morris JP, Wang SC, Hebrok M. KRAS, Hedgehog, Wnt and the twisted developmental biology of pancreatic ductal adenocarcinoma. Nat Rev Cancer. 2010;10(10):683-95.

61. Ji H, Ramsey MR, Hayes DN, Fan C, McNamara K, Kozlowski P, et al. LKB1 modulates lung cancer differentiation and metastasis. Nature. 2007;448(7155):807-10.

62. Spoerke JM, O'Brien C, Huw L, Koeppen H, Fridlyand J, Brachmann RK, et al. Phosphoinositide 3-Kinase (PI3K) Pathway Alterations Are Associated with Histologic Subtypes and Are Predictive of Sensitivity to PI3K Inhibitors in Lung Cancer Preclinical Models. Clinical Cancer Research. 2012;18(24):6771-83.

63. Kim J, Lee JJ, Kim J, Gardner D, Beachy PA. Arsenic antagonizes the Hedgehog pathway by preventing ciliary accumulation and reducing stability of the Gli2 transcriptional effector. Proceedings of the National Academy of Sciences. 2010;107(30):13432-7.

64. Kim J, Aftab Blake T, Tang Jean Y, Kim D, Lee Alex H, Rezaee M, et al. Itraconazole and Arsenic Trioxide Inhibit Hedgehog Pathway Activation and Tumor Growth Associated with Acquired Resistance to Smoothened Antagonists. Cancer Cell. 2013;23(1):23-34.

65. Stordal B, Davey M. Understanding cisplatin resistance using cellular models. IUBMB Life. 2007;59(11):696-9.

66. Patient-Derived Xenografts of Non Small Cell Lung Cancer: Resurgence of an Old Model for Investigation of Modern Concepts of Tailored Therapy and Cancer Stem Cells. Journal of Biomedicine and Biotechnology. 2012;2012:11.

# Biography

Lingling Huang was born on October 28th, 1986 in Guangxi province, China. She completed her preschool, elementary school, middle school and high school in Nanning city, Guangxi province, China. After the annual China College Entrance Exam in 2005, Lingling was accepted to the top 1 college in China: Tsinghua University (Beijing). In the summer of 2008, she attended a summer exchange program and obtained a certificate in Tohoku University, Sendai, Japan. In July 2009, she graduated from Tsinghua University with Bachelor of Science degree in Biological Sciences and Biotechnology.

In August 2009, she entered the Developmental and Stem Cell Biology program at Duke University, and became affiliated with the Molecular Cancer Biology program in 2010 to continue her Ph.D study. Since then, she has been working with Dr. Mark Onaitis and Dr. David Kirsch, focusing on oncogenic mechanisms of squamous lung cancer with the ultimate goal to identify novel and potent targeted therapies. In her five years in graduate school, she participates in various projects, attended two national conferences, and has published several research articles.

## EDUCATION

Duke University, Durham, NC, U.S.A, 2009-2014

Ph.D: Molecular Cancer Biology

Certificate: Developmental and Stem Cell Biology

Tsinghua University, Beijing, China, 2005-2009

B.S: Biological Sciences and Biotechnology

Tohoku University, Sendai, Japan, 2008

Certificate: Summer exchange program

## RESEARCH EXPERIENCE

Duke University, Department of Pharmacology and Cancer Biology, 2009-2014

Ph.D candidate: HH-GLI signaling in squamous lung cancer.

Advisors: Dr. Mark Onaitis, Dr. David Kirsch

Tsinghua University, Department of Biological Sciences and Biotechnology, 2007-2009

Student researcher: Signaling pathways in response to phosphate limitation in Arabidopsis.

Advisor: Dr. Dong Liu

## PUBLICATIONS

1. **Huang L**, Walter V, Hayes N, Onaitis M, Hedgehog-GLI signaling inhibition suppresses tumor growth in squamous lung cancer. *Clinical Cancer Research, Jan 14 2014. (Epub ahead of print)*

2. **Huang L**, Walter V, Hayes N, Onaitis M, GLI inhibition as a new strategy to treat lung squamous cell carcinoma (abstract). *In: Proceedings of the 2014 AACR-IASLC Joint*

*Conference on the Molecular Origins of Lung Cancer; 2014 Jan 6-9; San Diego, California. Philadelphia (PA): AACR; Clinical Cancer Research 2014; 20 (2 Suppl): Abstract nr A25*

3. **Huang L**, Walter V, Hayes N, Onaitis M, Inhibition of HEDGEHOG-GLI signaling suppresses tumor progression in squamous lung cancer (abstract). *In: Proceedings of the 2013 AACR-NCI-EORTC International Conference on Molecular Targets and Cancer Therapeutics; 2013 Oct 19-23; Boston, Massachusetts. Philadelphia (PA): AACR; Mol Cancer Ther 2013; 12(11 Suppl): Abstract nr B236*

4. Wang L, Li Z, Qian W, Guo W, Gao X, **Huang L**, Wang H, Zhu H, Wu JW, Wang D, Liu D, Arabidopsis purple acid phosphatase AtPAP10 is predominantly associated with the root surface and plays an important role in plant tolerance to phosphate limitation. *Plant Physiology November 2011 vol. 157 no. 3 1283-1299*

**CONFERENCES/ PRESENTATIONS**

1. 2014 AACR-IASLC Joint Conference on the Molecular Origins of Lung Cancer; 2014 Jan 6-9; San Diego, California. Invited Poster Presentation.

2. 2013 AACR-NCI-EORTC International Conference on Molecular Targets and Cancer Therapeutics; 2013 Oct 19-23; Boston, Massachusetts. Invited Poster Presentation.